

## 1. Introduction

In the fast evolving world we live in, time and money are two very important factors in the development of any system and more advanced technologies need to be developed in less time. Thus methods, which enable us to accomplish these new goals more rapidly, are essential.

In the automotive industry one of the methods used in accelerating the design, testing and development of systems and vehicles is the use of virtual vehicle simulations. Time is used more effectively when the simulations are run after hours and saves actual testing time. The simulations cut costs in the form of fewer prototypes required for actual testing and accelerated fault finding in the design of a system.

Simulation results are very dependent on the model used for the simulation as well as the inputs to the system. Viable results are often obtainable with a simplified model if the correct simplifications and assumptions are made together with accurate input data supplied to the simulation. This study concentrates on obtaining the input data, in the form of the terrain profile, used for vehicle simulations in which a vehicle is driving on rough terrains.

Thoresson (2003) developed and validated a mathematical model of the Land Rover Defender 110 used by the University of Pretoria as their test vehicle. The development of the 4 State Semi-Active Suspension System (4S<sub>4</sub>) was done by Els (2006) at the University of Pretoria and was implemented on the same Land Rover Defender 110. Rollover tests and simulations have been completed by Uys (2007) with the mathematical model developed by Thoresson with the addition of the 4S<sub>s</sub> suspension characteristics. Ride comfort simulations over the Belgian paving at the Gerotek Test Facilities completed by Thoresson did not correlate with the actual field tests, while correlation for the other obstacles were excellent. The conclusion was made that the Belgian paving data used in the simulations was imprecise and lead to the necessity of accurate profile information of the actual off-road terrains used in simulations and field tests.

The question of why measure actual roads when one can just generate a random road with the same Road Quality Index (RQI) or road roughness from the International Road Index (IRI) may be asked. The main reason why actual road information was required for this study remains for simulation verification and correlation with actual field tests. Each random road generated for a simulation differs and one was not able to execute and compare field tests on the same road. Off-road terrains are often not random and very little data on off-road terrains are available.

The main objective of this study is to obtain accurate profiles of actual off-road terrains used for vehicle testing at the Gerotek Test Facilities west of Pretoria, South Africa (Gerotek Test Facilities, 2007). The severe roughness of these terrains prevents the use of existing profilometers available in South Africa.

The terrains are cast in concrete, kept in good condition and are only used for testing and not driven on continuously. These terrains are used as the benchmark for testing by many commercial, military and off-road vehicle developers. From these profiles realistic three dimensional (3-D) models are generated. The 3-D models are then used in virtual vehicle simulations. This is done in order to correlate the response of the vehicle in virtual simulations with real life tests.

Three different methods are considered in measuring the profile of the terrain. The first method is a mechanical measuring device nick named the Can-Can Machine, the second method utilizes Photogrammetry and the third method is a laser which scans a section of the terrain at a time. These methods are evaluated by profiling the same section of the Belgian paving at the Gerotek Test Facility (Gerotek Test Facilities, 2007) and calculating the Displacement Spectral Densities. The most efficient method is used to profile more terrains used for actual testing and in turn used in simulations. Simulations assist in the development and improvement of vehicle suspension systems and set-ups. The results from the simulations are correlated with actual tests done on the same terrain using a previously validated MSC.ADAMS/VIEW model of a Land Rover Defender 110, Thoresson (2003) and Els (2006).

A brief literature overview concerning on-road and off-road profilometers used in the past and present, together with statistics and profile characterisation methods are presented in paragraph 2. The development, working principals, testing and calibration of suitable equipment of three different profilometers are discussed in paragraph 3. In paragraph 4 simple obstacles are profiled and evaluated. The profiling of 3-dimensional rough roads are presented, discussed and characterized in paragraph 5. In paragraph 6 off-road simulations and results are presented and discussed. Conclusions drawn from the study together with recommendations for future work are presented in the final paragraph.

## 2. Literature survey

Realistic terrain representation is the key to successful physics-based simulations of all-terrain, all-season vehicle performance, (Shoop et.al., 2004). The use of 3-D tyre models in simulations are increasing and thus 3-D road profiles are required. In 3-D simulations the road is sometimes modelled as separate left and right surfaces to reduce the number of elements in contact with the tyre, as it reduces the solver duration.

Imine et.al (2003) describes a profilometer as an instrument used to produce a series of numbers related in a well-defined way to a true profile. Gorsich et.al. (2003) states that road profilometers typically has errors caused by gyro errors and errors caused by ultrasonic devices. Low frequency trends in the data were often removed using a high pass filter. Other errors were caused by the dynamics of the vehicle carrying the profilometer and the road profilometer itself. Some road profilometers only take a one-dimensional trace (or two traces) of the three-dimensional surface of the road. This removes all the lateral variation in the data, and assumes every time a vehicle drives along the road or terrain, it drives along exactly the same path. On a typical test course, different paths mean different road profiles and possibly much different reliability and durability results. The fact that different paths mean different road profiles embraces the requirement for accurate full 3-D terrain profiles for valid simulation results.

In the above references, no indication was provided to which profilometer had been used in obtaining data on roads. Concrete and asphalt roads are also referred to as smooth or normal roads due to the fact that these roads are extensively smoother than the off-road terrains which need to be profiled for the current study.

### 2.1. *Road profilometers*

The following paragraphs describe different profilometers and profiling methods employed in recording the profiles of concrete or asphalt roads.

#### 2.1.1. High Speed Profilometers (HSP)

The Council for Scientific and Industrial Research (CSIR) is one of the largest research, technology and innovation institutions in Africa. In profiling a road the CSIR utilizes a High Speed Profilometer (HSP), as seen in Figure 1 (Anon, 2005).

The HSP can collect accurate information relating to the longitudinal and transverse variations of a road surface relatively quickly. The HSP measures:

- Longitudinal profiles in both wheel tracks at 250 mm intervals;
- Transverse profiles spanning both wheel tracks (lane occupied by vehicle) at regular intervals down to 1,5 m;
- Geographic coordinates by means of GPS accurately to within one metre;
- Longitudinal gradients.

The HSP is a sophisticated instrument using modern laser and optical technology and it can test at speeds up to 120 km/h.



**Figure 1: The HSP of the CSIR (Anon, 2005).**

The same type of equipment used by the CSIR is used in the United States of America, which also just profiles the wheel tracks of the vehicle used to transport the profilometer. An assessment of profilometer performance for construction quality control was done by the University of Michigan Transportation Research Institute (UMTRI), (Karamihas and Gillespie, 2002). The assessment was performed on four sites: (1) moderately rough asphalt of typical surface texture, (2) new longitudinally tined concrete, (3) moderately rough broom-finished concrete and (4) new transversely tined concrete. Four broad classes of profilometers participated in the assessment. They were as follows: Static, Walking-speed, Lightweight Inertial and High-speed Inertial Profilometers.

The Walking-speed and Lightweight Inertial Profilometers fundamentally work on the same principals as the High-speed Inertial Profilometers. The Inertial Profilometer will be discussed in paragraph 2.1.2.

Figure 2 and Figure 3 show the difference between the longitudinally tined concrete and the transversely tined concrete respectively. It is clear that these surfaces are considered rough when one's hand is brushed over it. The intension of the present study is to profile off-road terrains, where the range of the vertical displacement on the road can vary from 10 mm up to 150 mm.



**Figure 2: Longitudinally tined concrete, direction of travel from bottom to top (Karamihas and Gillespie, 2002).**

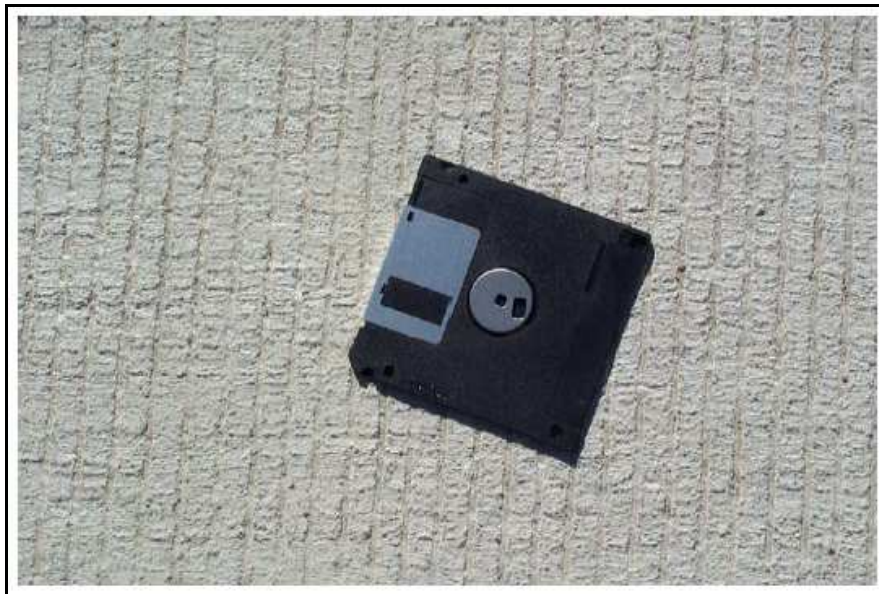


**Figure 3: Transversely tined concrete, direction of travel from left to right (Karamihas and Gillespie, 2002).**

## 2.1.2. Inertial Profilometer

General Motors Research Laboratories made a breakthrough in the 1960's when they developed the Inertial Profilometer. This made high-speed profiling possible for monitoring large road networks (Spangler, 1964).

According to Spangler (1964) an Inertial Profilometer utilizes an accelerometer which measures the vertical response of the vehicle travelling on the road. The profilometer was capable of measuring and recording road surface profiles at speeds ranging from 16 to 112 km/h. The vertical body motion (Inertial reference) was obtained by the double integration of the response measured by the accelerometer.

The relative displacement between the pavement surface and the vehicle body was measured with a non-contact light (laser) or acoustic measuring system (Infrared or ultrasonic sensor) and was mounted on the vehicle body together with the accelerometer. Figure 4 shows a schematic drawing by Imine and Delanne (2005) of an Inertial Profilometer.

The pavement elevation profile was obtained by subtracting the output from the height sensor from the absolute motion of the vehicle body (Kulakoski et.al., 1986).

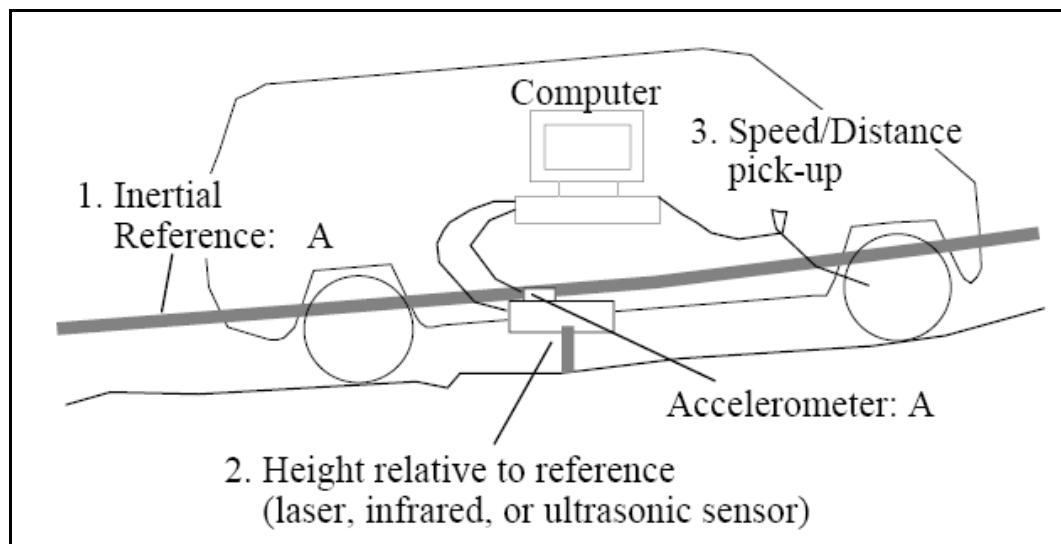


Figure 4: Schematic drawing of an Inertial Profilometer by Imine and Delanne (2005).

Imine and Delanne (2005) removed the noise in the acceleration signal by filtering the signal with a low-pass filter. A high-pass filter was then used to eliminate the low-frequency component and constant generated by the integration of the acceleration signal.

As stated previously the Lightweight Profilometer and the Walking Profilometer were variations on the High Speed Profilometers but they were essentially based on the principals of the High Speed Profilometer. Karamihas and Gillespie (2002) indicated that Lightweight Inertial Profilometer and High Speed Inertial Profilometer measurements were supposed to have the same meaning. This was very important for several reasons: (1) High Speed Profilometers were often used to audit measurements made by Lightweight Profilometers for smoothness specifications, (2) High Speed Profilometers may be used for measurements of smoothness of pavements that were under warranty, and (3) studies of roughness progression from cradle to grave often rely on measurements by both types of Inertial Profilometer. Examples of these profilometers can be seen in Figure 5 and Figure 6 respectively.



**Figure 5: International Cybernetics Corporation Lightweight Profilometer, profiling moderately rough asphalt (Karamihas and Gillespie, 2002).**



Figure 6: Walking Profilometer (Karamihas and Gillespie, 2002).

### 2.1.3. Longitudinal Profile Analyser

The Longitudinal Profile Analyser (Figure 7), also known in French as APL has been developed by The Roads and Bridges Central Laboratory (Imine and Delanne, 2005). The system includes one or two signal-wheel trailers towed by a car at a constant speed. A data acquisition system was utilised to record the data. An oscillating beam holding the measuring wheel was supported by a chassis and a suspension and damping system ensures that the wheel was in permanent contact with the pavement.

Vertical movement of the wheel results in angular travel of the beam, measured with respect to the horizontal arm of an inertial pendulum, independently of movements of the towing vehicle.

An angular displacement measurement was made with the use of an angular displacement transducer associated with the pendulum. The electrical signal was amplified and recorded by the data acquisition system. Rolling surface undulations in a range of 100 mm were recorded, for wavelengths in ranges from 0.5 to 20 m or 1 to 50 m, depending on the speed at which the chassis was towed.



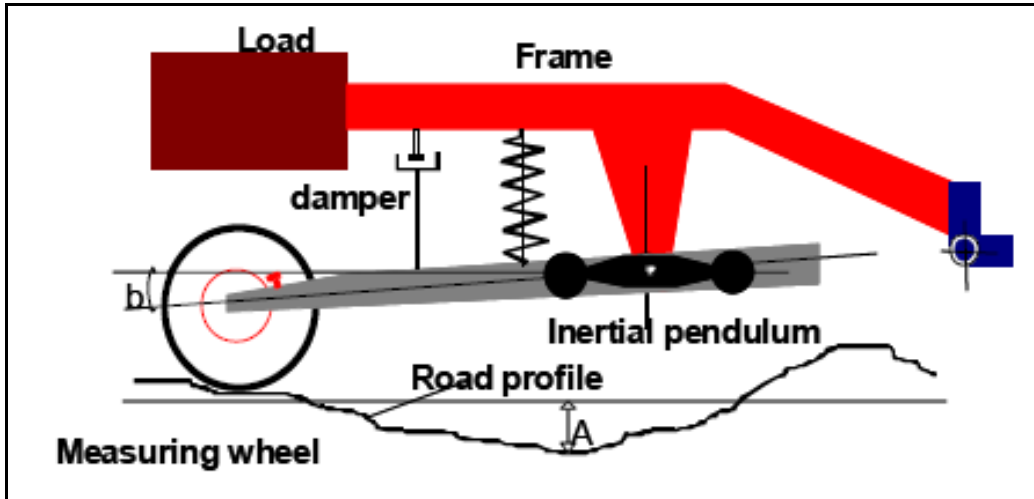


Figure 7: Longitudinal Profilometer Analyser (Imine and Delanne, 2005).

Imine and Delanne (2005) proved that the Longitudinal Profilometer Analyser gave a very precise measurement of the profile elevation. Rough measurements had to be processed to get a good estimate of the road profile.

## 2.2. Off-road Profilometers

The following methods were used in obtaining profiles for off-road terrains which were sometimes referred to as rough roads. These methods may also be used on normal/smooth roads.

### 2.2.1. Rod and Level

The rod and level are familiar surveying tools. This method is called “static” because the instruments are stationary when the elevation measures are taken (Sayers and Karamihas, 1998).

The elevation reference is provided by the level, the readings from the rod provide the height relative to the reference and a tape measure locates the individual elevation measurements. The method is shown in Figure 8.

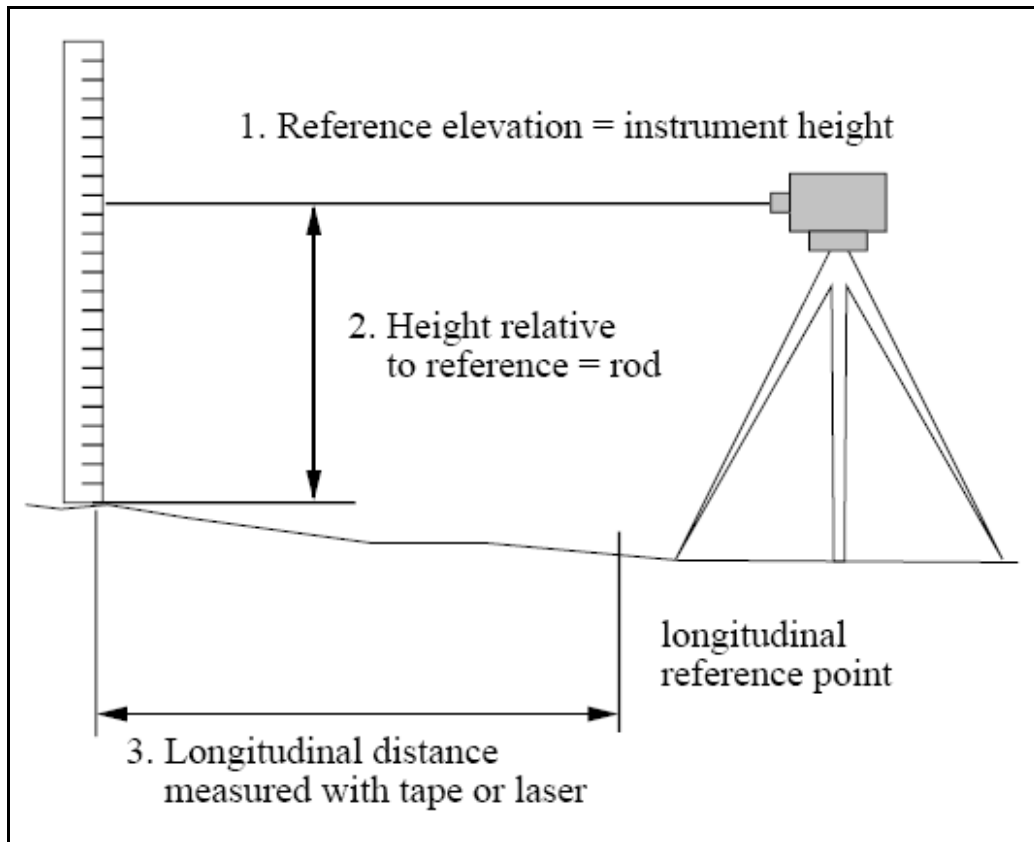


Figure 8: Visual representation of the Rod and Level Profilometer (Sayers and Karamihas, 1998).

This method is generally used for laying out a road. The requirements for obtaining a profile measure that is valid for computing roughness differ in that the elevation measurements need to be taken at close intervals of 250 mm or less (Sayers and Karamihas, 1998). This can be a very time consuming exercise and are much more stringent than necessary for normal surveying. The ASTM Standard E1364 provides guidelines for measuring profiles with a static method (ASTM E1364 – 95, 2005).

### 2.2.2. The Dipstick

In the Little Book of Profiling (Sayers and Karamihas, 1998), the Dipstick, see Figure 9, is described as a device developed and patented by the Face Company. The device is faster than the rod and level method in measuring profiles of roads suited for roughness analysis. It includes a battery-powered computer which automatically records data and performs the arithmetic needed to produce a profile.

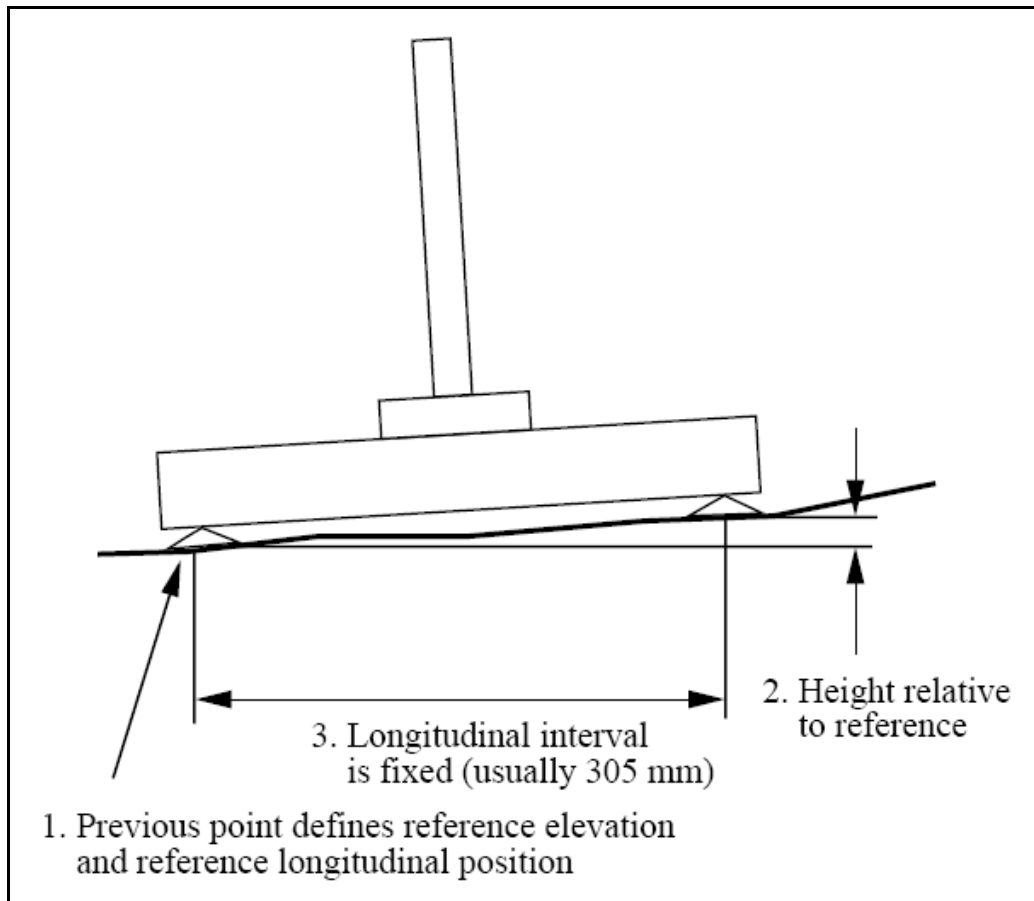


Figure 9: A basic representation of the Dipstick (Sayers and Karamihas, 1998).

The device is “walked” along the line being profiled. It contains a precision inclinometer that measured the difference in height between supports. The base on which these supports were mounted were normally spaced 305 mm apart. A line along the ground was profiled as follows: lean the device forward so that all of its weight is on the leading foot, raising the rear foot slightly off the ground. Pivot the device 180° about the leading foot, locating the other foot (formerly behind the leading foot) in front, along the line being profiled. The sensor was constantly monitored by the computer. When the computer senses that the instrument has stabilized, it automatically records the change in elevation and beeps; this signals that the next step may be taken.

The reference elevation in this design was the value calculated for the previous point. The height relative to the reference was deducted by the angle of the device relative to gravity, together with the spacing between its supports. The longitudinal distance of the profile was calculated by multiplying the number of measures made with the known spacing of the supports.

The profiles obtained with the Dipstick and the profiles obtained with the Rod and Level typically correspond to one another if the value of the first elevation (the initial reference) was set to match the elevation used in the Rod and Level profile.

### 2.2.3. Vehicle Terrain Measurement System

The Vehicle Terrain Measurement System (VTMS), (Kern, 2007), consists of four major components: a scanning laser, an inertial navigation system, a data acquisition system and a power management system. The use of these components allows this system to record the measured profile and to place the profile in global coordinates. These components are mounted on the rear of the host vehicle as shown in Figure 10. The VTMS is capable of measuring profiles both on-road and off-road.

The scanning laser is mounted 2 m above the profiled terrain and scans the terrain surface over a width of 4 m. The spacing between sequential points in the grid is approximately 5 mm, however the spacing is not uniform. This is due to the scanning laser operating by directing a laser beam at a rotating prism. The rotation of the prism causes the reflection of the laser beam to the terrain to be in equally spaced angles across the width of the scan. This causes the spacing in the centre of the path to be about 3.3 mm and 6.6 mm on the outside of the path. A second cause is that the lateral position depends on the vertical position of each point.



Figure 10: Vehicle Terrain Measurement System mounted on host vehicle (Kern, 2007).

The positioning system used in the VTMS is a Differential Global Positioning System (DGPS). The DGPS produces global positioning with an accuracy of 20 mm for a longitudinal distance traveled up to 10 km. Thus the final accuracy of the Vehicle Terrain Measurement System is confined to the 20 mm accuracy of the DGPS. The DGPS consists of two units, the base unit which is stationary and the unit mounted in the host vehicle, which contribute to the accuracy obtained. The DGPS signal is then combined with the IMU measurements in a Kalman filter to produce the final prediction of the orientation and position of the host vehicle.

#### **2.2.4. Profilometers used in South Africa for profiling off-road terrain**

Zaayman (1988) developed a tool for measuring and characterizing the profiles of rough terrain surfaces. A workable measuring device was created which would need only minor modifications for it to be applicable to a large variety of terrains. The measuring device was complete with software which was developed to give a set of profile heights for the measured terrain. The profile characterization software calculated the power spectral density of the profile as well as the roughness constant.

The system comprised of hardware components linked to measurement instrumentation and software. The hardware consisted of a two wheeled cart which had a small single wheel following the left hand track of the vehicle and a wheel-set following the right hand track of the vehicle (see Figure 11). The wheel-set was constructed in such a way that there were always at least two wheels following the ground in the track profile. The pivot movement of the wheel-set with respect to the cart frame was measured by a potentiometer giving as output the angle  $\alpha$  between the wheel-set frame and the cart frame. A proximity switch was mounted on the wheel-set, with a notched plate attached to one of the wheels, thus a pulse was generated every time the notched plate passed the proximity switch during movement.

This gave the sloped distance which the cart had covered. In order to ensure that the wheel constantly turned, even though it might not have been in contact with the ground, the front and rear running wheels were connected by a chain and sprocket system.

A gyroscope mounted on the cart frame measured the pitch angle  $\theta$  and roll angle  $\beta$  which the frame made with the absolute horizontal plane as it moved behind the towing vehicle. The values of  $\theta$ ,  $\beta$  and  $\alpha$  were recorded every time a pulse occurred in the signal of the proximity switch. The output signals from every transducer were stored on an FM tape recorder.

The coordinates were then converted to only the value of the height,  $y$ , at equally spaced horizontal distances. The result was an array of height values,

y, starting at horizontal distance  $x = 0$  which could be plotted to form the profile of the road.

The smallest obstacle the concept could measure with reasonable accuracy was a half round obstacle with the radius equal to the radius of the wheel (37 mm).

The speed of the tow vehicle could not be kept at a low enough speed for rough terrains. Too high towing speed resulted in the proximity switch generating pulses too fast and the pulses could be missed during analogue to digital conversion of the time data. The higher towing speed also generated unwanted vibrations and movement of the measuring device.

This concept worked better for the profiling of tarred roads where the amplitude of the longitudinal displacement of the surface was small in comparison with those found on off-road terrains. The concept also only measured a single line on the road travelled.

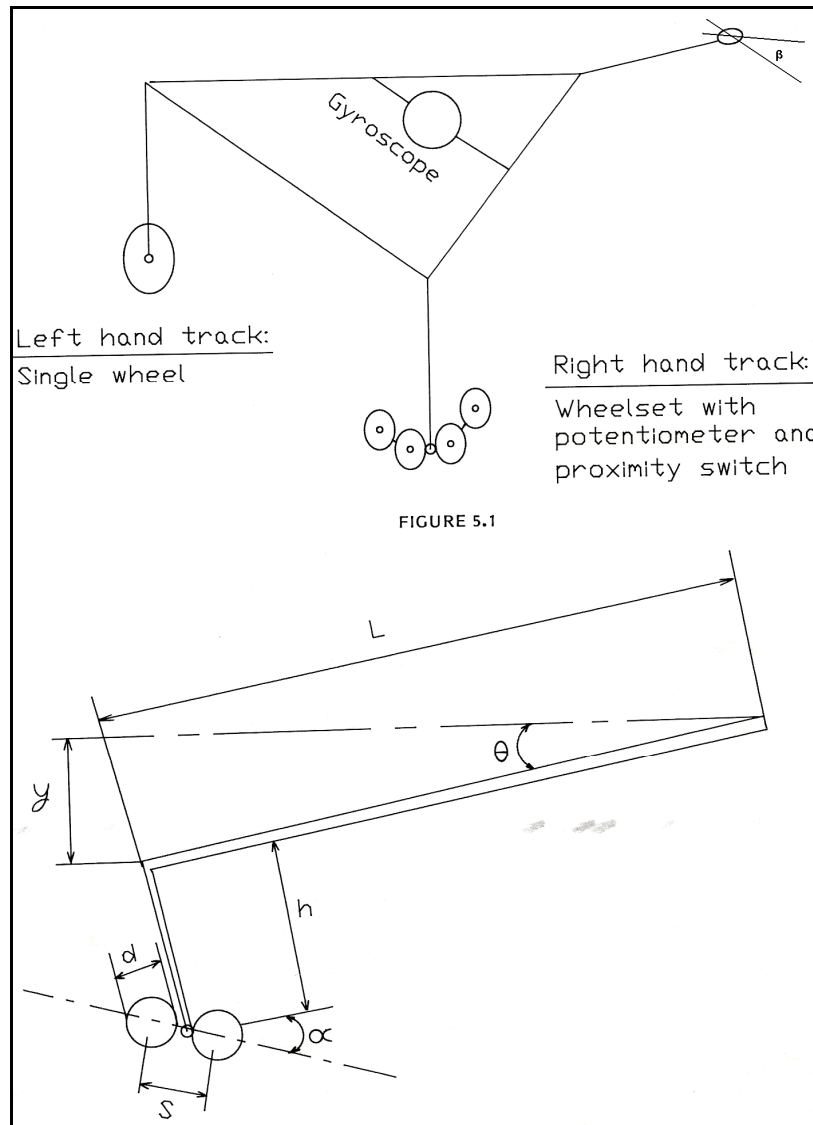


FIGURE 5.1

Figure 11: Zaayman's description of his concept (Zaayman, 1988).

### 2.3. Stereo Vision Measurement System

The experimental stereo vision system of the Sheffield Centre for Earth Observation Science (SCEOS) as described by McDonald et.al. (2000) comprises of two CCD cameras, a mount and a frame grabber connected to a computer (see Figure 12). It is possible to measure the position of an object by placing the object in view of both cameras. The cameras are focused on the object and the images are recorded. The simultaneous recording of the images are done with the use of the TINA software tool as described by Pollard et.al. (1989). The edge detection algorithm, as described by Canny (1986), is used to detect the position of the edges for each of the two images. The calibration process, which is done with a calibration tile, yields sixty-four

constraints on the seven camera parameters which include a translation vector, three angles of rotation and a focal length. The software uses the information on the edges of the images along with the camera parameters obtained from the calibration to rectify the stereo images to a parallel camera configuration.

The edge features in the rectified images are then correlated to determine the relative positions of the pixels in each image. The positions of the correlated pairs of pixels in the rectified image are then triangulated to determine the position of the particular points on the soil surface with reference to the position of the left camera. To aid the correlation procedure, which can become confused when noisy images are used, a laser stripe generator is used to produce one distinct line in the pair of images.

The best way to measure a soil surface is to take several sets of stereo images offset by a known amount; a mosaic of the images can then be used to produce useful measurements of the soil profile at the required resolution. The movement of the cameras and laser are constrained to one dimension to ease the alignment process. This is done by mounting the CCD camera and laser diode on a linear scanner. The movement of the system is regulated by a computer controlled stepper motor over a length of three metres. The accuracy of the profilometer is dependent on the resolution of the CCD camera, the integrity of the reference and soil images, the alignment and the positional accuracy of the linear scanner.

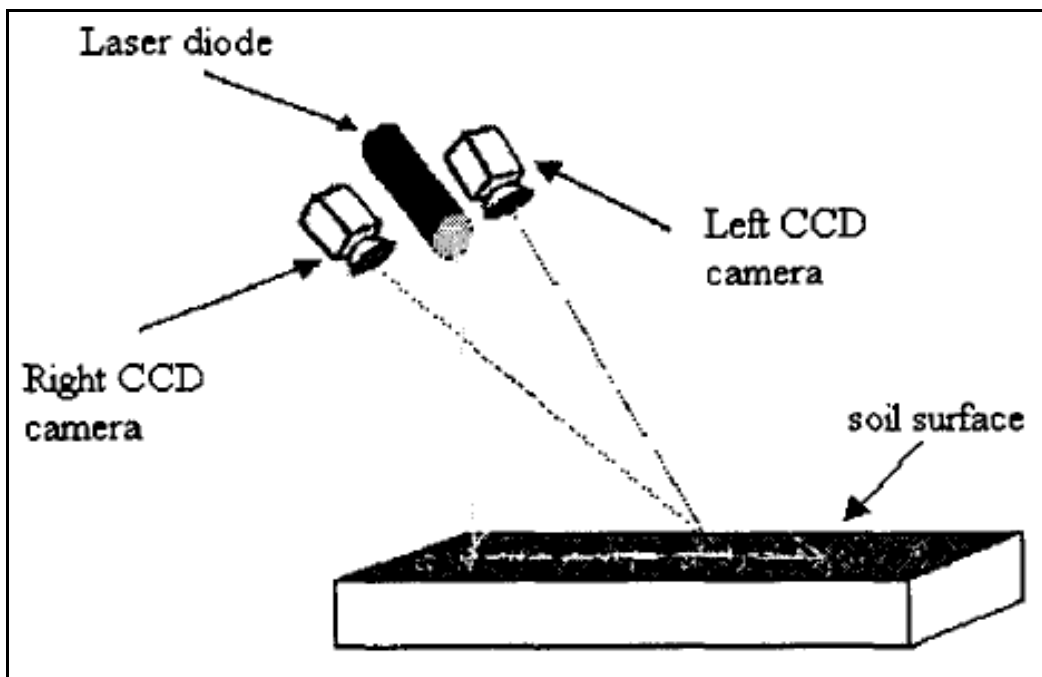


Figure 12: A schematic view of the Stereo Vision Measurement System (McDonald et.al., 2000).



## **2.4. Aerial Photography**

Man's ability to see in three dimensions is a result of having two eyes that record slightly different images of the objects around him. These two slightly different images are fused by the brain to give an impression of depth.

An essential feature of aerial photography for mapping purposes is that it must be possible to view an optical model of the terrain in three dimensions. If the photographic sequence is arranged so that a portion of the terrain between the two camera stations is recorded on successive exposures, two slightly different views of the same area of terrain, called the 'overlap', are recorded on the photographic emulsion. If the pair of photographs, also known as stereo pairs, is viewed under suitable conditions, an optical model of the area of overlap will be seen in relief. The condition to be satisfied is for each eye to have a slightly different view of the same area of terrain; this can be achieved if the left eye only views the left photograph and the right eye views only the right photograph of the overlap (see Figure 13) (Ritchie et.al., 1991).

A three-dimensional, or stereoscopic, image of the terrain cannot be created from aerial photographs unless the conditions, as described above, are reproduced in their taking. The dimension of height not only enhances the interpretation of many features but also allows the photogrammetrist the possibility of measuring heights within the stereoscopic model, using only a minimal amount of ground-derived information. Normally four known height points are required for one overlap. Figure 14 describes the overlap requirements for complete photographic coverage.

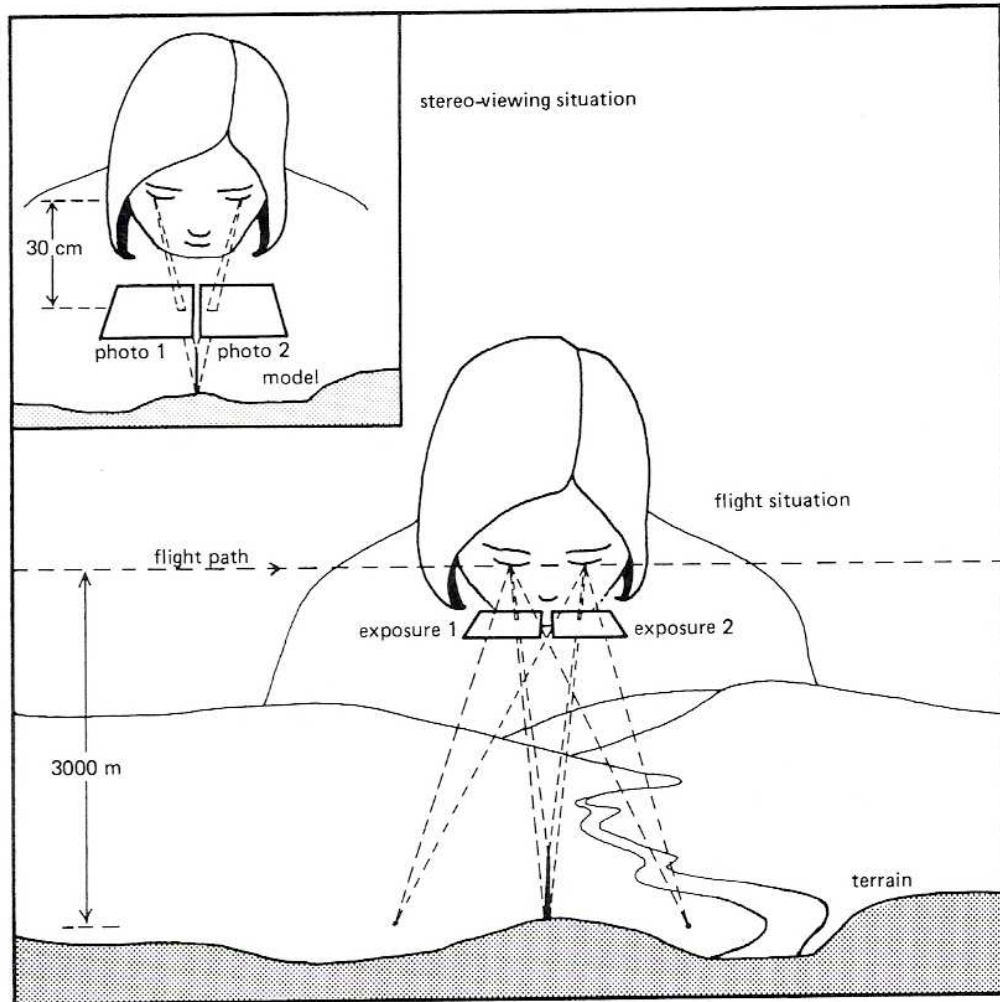


Figure 13: Giant eye-base described by Ritchie in *Surveying and mapping for field scientists* (Ritchie et.al., 1991).

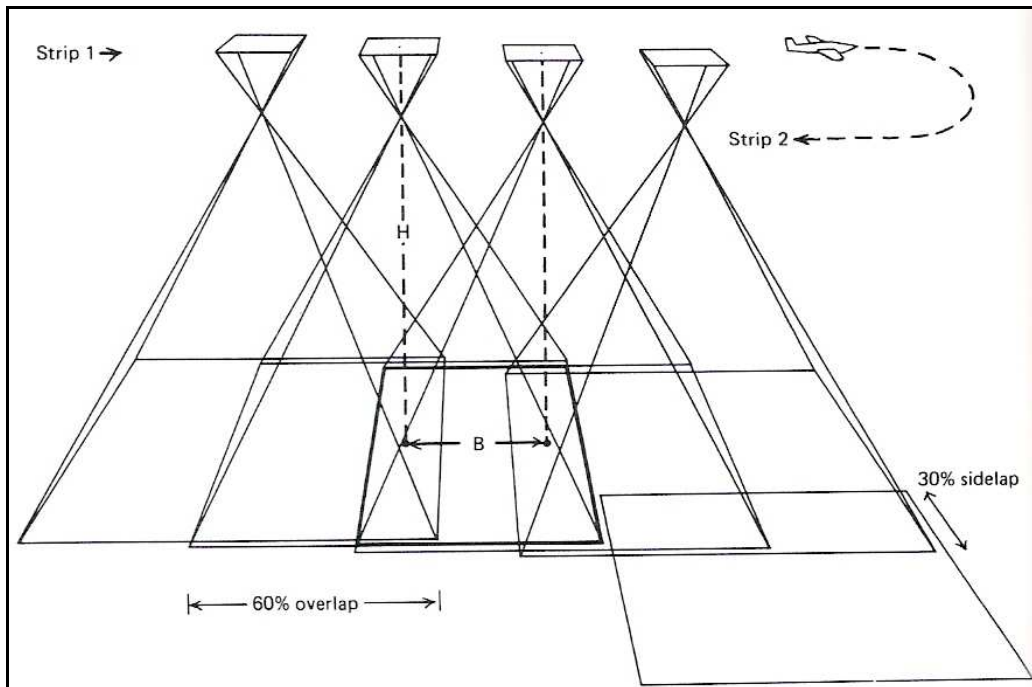


Figure 14: Overlap requirements for complete photographic coverage and stereoscopic viewing described by Ritchie (1991).

## 2.5. Stereoscopes

The simplest, and least expensive, piece of equipment for viewing the three-dimensional image from overlapping photographs is the lens stereoscope. It consists of a pair of lenses mounted on a frame, which is supported over the photographs by thin metal legs. Figure 15 shows two examples of stereoscopes.

When the lens stereoscope is set up, the distance from the lens to the photograph is equal to the focal length of the lenses, so that the photographic image will appear sharp in the focal plane of the lenses. The image appears enlarged, usually 2x to 2.5x. The photographs are arranged below the lenses so that the appropriate eye is viewing the same detail in the appropriate photograph at the same time. It is necessary to place one photograph on top of the other so that the separation of corresponding images is about the same as the lenses separation. This limits the portion of the photograph that can be viewed at any time. The portability of the lenses stereoscope makes it suitable for use in the field.

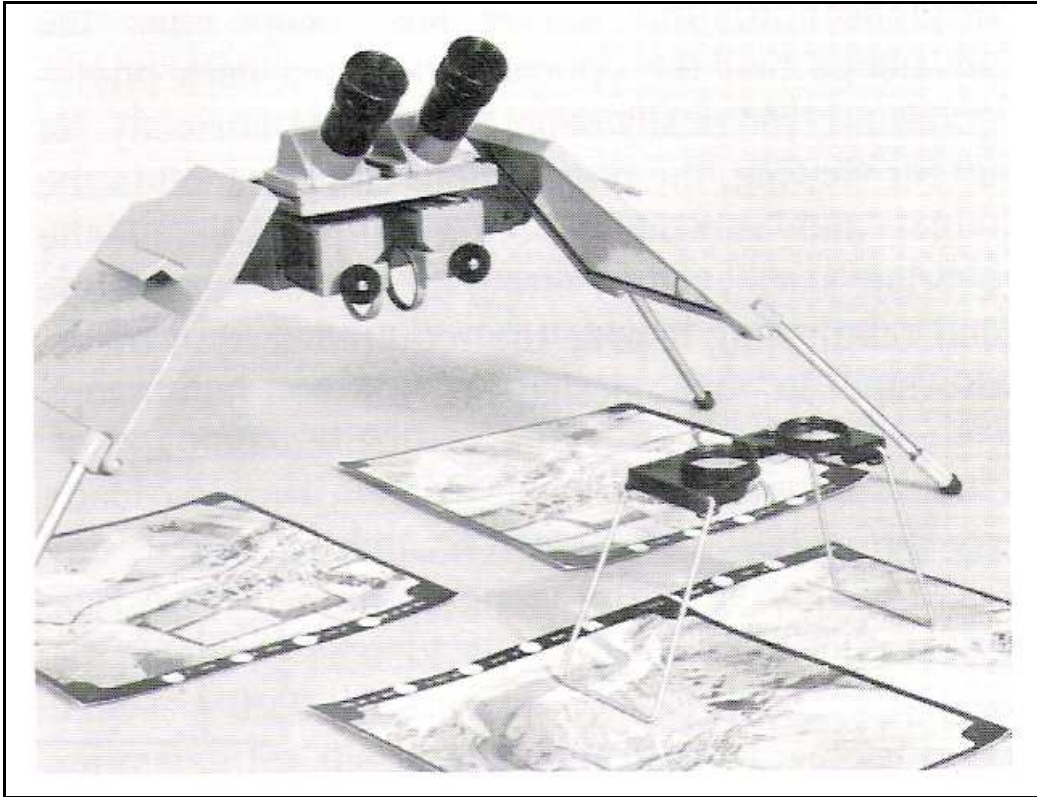


Figure 15: Mirror stereoscope and lens stereoscope (Ritchie et.al., 1991).

## 2.6. *Laser Displacement Scanners*

Several groups have been studying the best way to acquire 3-D models of real world environments. Research efforts generally fall into one of two categories: image-based methods, where the 3-D geometry is inferred from 2-D images; and the laser range-based approach, where the 3-D geometry is measured directly through laser range scanners.

Image-based methods have been around the longest and have been used for many 3-D modelling tasks. The standard method for developing large-scale terrain models is with the use of stereo techniques with aerial imagery to develop coarse models of the ground below, as described in Paragraph 2.3 to 2.5.

The MIT City Scanning Project uses spherical cameras and Geographic Information System (GIS) localization to develop models of the environment around them. In general, these techniques give results that have centimetre-to metre-level accuracy. Other laser sensor platforms are available which produce geo-referenced imagery but they produce data that is not suitable for close-range mapping, (Antone and Teller, 2000).

The University of Tennessee, Knoxville (UTK) developed a Mobile Scanning System which is more flexible in the types of environments and structures that can be digitized when compared to methods utilizing aerial terrain scanning. Their system combines laser range scanners, high resolution video cameras, a Global Positioning System (GPS) and an Inertial Navigation System (INS) to measure the system's position and orientation. The instrumentation is mounted on a vehicle and the terrain is digitized to provide a geometrically accurate 3-D model of the terrain as the vehicle is driving, an example of the vehicle is shown in Figure 16. The system uses a downward looking laser range scanner to digitize the terrain.



**Figure 16: UTK's Mobile Scanning System consisting of a vehicle, laser range scanner, GPS, INS and high-resolution video camera (Grinstead et.al., 2005).**

The Mobile Scanning System acquires data in real-time but processes the data offline. A typical terrain model can consist of over 200 000 geometry profiles, 1 million position and orientation measurements and 20 000 high resolution colour images. A rough estimation of the storage capacity required for the raw data alone exceeds 10 gigabytes.

The micro-scale system utilizes an Integrated Vision Products (IVP) Ranger to acquire high-resolution, high-accuracy 3-D models of roads and other surfaces. The measuring principle of IVP Ranger to acquire 3-D shapes is based on the method called laser triangulation, or sheet-of-light range imaging. The object is illuminated from one direction with a laser line projector and viewed with the camera from another. The illumination angle, the viewing angle, and the baseline between the illuminator and the camera define the triangulation geometry, from which the camera calculates the 3-D shape. The micro-scale system is capable of measuring the geometry very densely

(approximately 1 mm between data points) with an accuracy on the order of 5 mm, at the cost of having a very limited field-of-view and a high amount of raw data to process (Grinstead et.al., 2005).

## **2.7. Road Profile statistics**

An extensive amount of work has been conducted by, amongst others, Sun et.al. (2005), Gorsich et.al. (2003) and Rouillard et.al. (2001) on obtaining statistical information on actual roads. Statistical models of each test terrain at the US Army's Aberdeen Test Centre have been created to establish and quantify the roughness of each course. The assumptions of linearity, normality and stationarity are usually made about a time series in order to create proper models for course elevations. Stationarity means that the variation of the course is uniformly rough along the length of the course. Linearity is essential for a relatively simple representation of the series. Normality is a common assumption used to build statistical models.

Sun et.al. (2005) tested stationarity by comparing the mean and the variance for the different segments of the data. A previous study indicated that the Belgian Block data is linear and Gaussian but not stationary.

The statistics are also used when random roads are generated from a given Road Quality Index (RQI) or road roughness from the International Road Index (IRI). Each random road generated for a simulation differs and one is not able to execute and compare field tests on the same road. Off-road terrains are often not random and very little data on off-road terrains are available. The focus of this study is on the off-road terrains at the Gerotek Test Facilities (Gerotek Test Facilities, 2007), whose profiles are not known. The emphasis on the present study is not on obtaining statistics of the profiles, but rather real terrain profiles for the use in simulations.

## **2.8. Displacement Spectral Densities (DSD)**

The roughness of a test course can be specified with the use of the Root Mean Square elevation (RMS) in the time domain or a Displacement Spectral Density (DSD) in the frequency domain (Gorsich et.al., 2003), and the roughness of a terrain is characterized according to the ISO 8608 standard, ISO (1995). The RMS of the vertical displacement of the profile and the square root of the area under the displacement spectral density should result in the same value.

The Power Spectral Density (PSD) of a signal describes how the power of a signal or a time series is distributed in the frequency domain. The same can be done for the displacement; consequently the Displacement Spectral

Density of a signal describes how the displacement of a signal or a time series is distributed in the frequency domain.

The ISO 8608 standard, ISO (1995), is an international standard which specifies a uniform method of reporting measured vertical road profile data for either one-track or multiple-track measurements. It applies to the reporting of measured vertical profile data taken on roads, streets and highways and on off-road terrain. The standard provides general guidance for the use of road profile statistical data for simulation studies and for related studies such as evaluation of comfort, suspensions and road profiles. The ISO standard supplies one with different road classifications, these classifications are supplied in the form of class limits for the Displacement Spectral Densities for different classes of roads. The classes range from a class-A road which is a smooth road to a class-H road which is a very rough terrain. The classes are presented on a graph as shown in Figure 17.

The earliest motivation for performing Displacement Spectral Density calculations on road profiles was their usefulness in vehicle dynamics. However, many researchers noted that the Displacement Spectral Density would also be a convenient way to classify road roughness and deterioration, (Andren, 2006).

The estimated Displacement Spectral Density is formed by taking the Fast Fourier Transform (FFT) of a window of the now one-dimensional processed profile. Windowing the data on a segment of the road profile data allows multiple estimated Displacement Spectral Densities to be formed and averaged to increase the accuracy of the final Displacement Spectral Density. The windowing is typically done with a Hanning window. Changing the window sizes can also greatly vary the final Displacement Spectral Density estimate Gorsich et.al. (2003).

The Displacement Spectral Density of a random road, plotted on a log-log scale, formulates a straight line and may be described by the power function.

$$S_z = A\varphi^{-n}$$

Where  $S_z$  is the vertical displacement spectral density (mean vertical displacement)<sup>2</sup> / (frequency band),  $n$  is the road index,  $A$  is the roughness coefficient at a spatial frequency of 1 cycle/m and  $\varphi$  is the spatial frequency measured in cycles/metre (cycles/m), Uys et.al. (2007). The road index parameter is calculated with a spatial frequency window from 0.05 cycles/m to 10 cycles/m.

The ISO 8606 standard (ISO, 1995) specifies that for off-road profiles the reported spatial frequency range for  $\varphi$  should be from 0.05 cycles/m (wavelength = 20 m) to 10 cycles/m (wavelength = 0.1 m).

Hall (1998) indicated that the lower value of  $\varphi = 0.05$  cycles/m was accepted since the vehicle speed over off-road/ rough terrain was normally much less

than the case for on-road terrains. The upper spatial frequency limit of  $\phi = 10$  cycles/m was consistent with the length of the tyre contact patch.

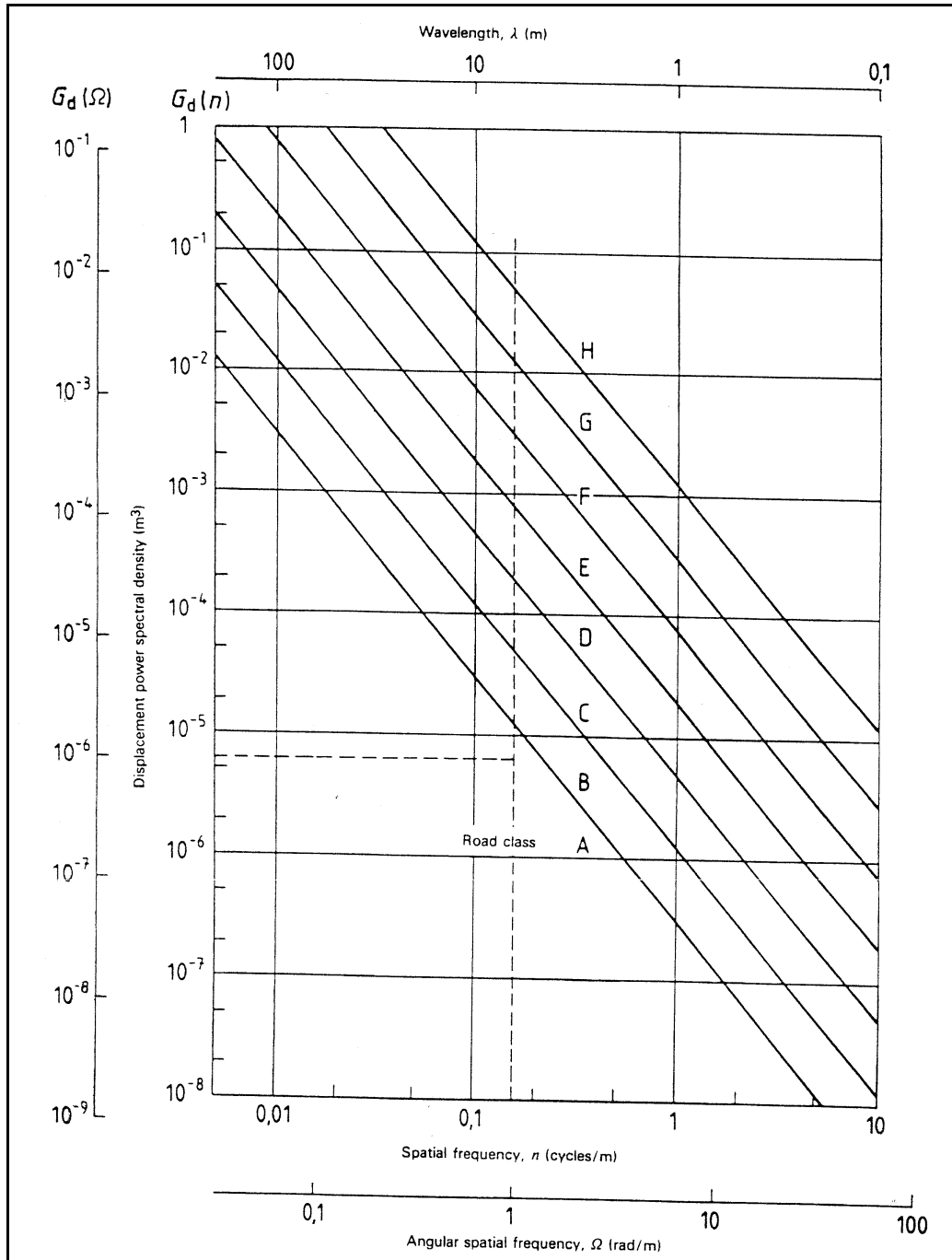


Figure 17: ISO 8606 road classification, (ISO, 1995).

Road profiles are usually considered to be a random process  $x(d)$ , where  $x$  is the road height and  $d$  is the distance along the road. As the vehicle travels along the road with a velocity  $v$ , the random process  $x(d)$  is converted to a



random process in the time domain  $x(t)$ , which is the input to the vehicle suspension via the tyre. The process  $x(d)$  is generally described in terms of its Displacement Spectral Density as a function of the frequency in either radians or cycles per unit distance. A stationary zero mean random process  $x(t)$  with dimensions of distance (m) can be characterized by its autocorrelation function:

$$R_{xx}(\tau) = \langle x(t)x(t-\tau) \rangle = \lim_{T \rightarrow \infty} \frac{1}{T} \int_0^T x(t)x(t-\tau) dt \quad [\text{m}^2]$$

where  $\langle x(t)x(t-\tau) \rangle$  is the time averaging operation.

If  $f$  is the frequency variable in cycles per second or more commonly known as Hz, the 'double side' Displacement Spectral Density  $S_{xx}(f)$  is the Fast Fourier Transform of the autocorrelation function  $R_{xx}(\tau)$ .

$$S_{xx}(f) = \int_{-\infty}^{\infty} R_{xx}(\tau) e^{-j2\pi f\tau} d\tau \quad [\text{m}^2/\text{Hz}]$$

The Displacement Spectral Density has the property that if the integral is calculated over all of the frequencies, the mean square value of  $x(t)$  is determined.

A road profile  $x(d)$ , with  $d$  being the distance along the road, can be characterized by the autocorrelation function  $R_{xx}(\delta) = \langle x(d)x(d-\delta) \rangle$ , where  $\langle x(d)x(d-\delta) \rangle$  is now a distance averaging operation. The Displacement Spectral Density of the road profile  $x(d)$  which is still determined with the use of the Fast Fourier Transform of the autocorrelation function,  $R_{xx}(\delta)$ , is then expressed in terms of a frequency variable  $F$  in cycles per metre (Davis and Thompson, 2001).

$$S_{xx}(F) = \int_{-\infty}^{\infty} R_{xx}(\delta) e^{-j2\pi F\delta} d\delta \quad [\text{m}^3/\text{cycle}]$$

Another valid method for calculating the Displacement Spectral Density was described by Zaayman (1988). In this method the Displacement Spectral Density  $S_{xx}(\delta)$  of the road was calculated by dividing the squared Fast Fourier Transform  $X_\delta$  of the road profile  $x(d)$  by twice the step in frequency  $\Delta F$ .

$$S_{xx}(F) = \frac{|X_{\delta}(F)|^2}{2\Delta F}$$

The squared Fast Fourier Transform is equivalent to the Fast Fourier Transform of the road profile  $X_{\delta}$  multiplied with the complex conjugate of  $X_{\delta}$ .

$$|X_{\delta}(F)|^2 = X_{\delta}X_{\delta}^*$$

This method used in calculating the Displacement Spectral Density is accurate and is used for calculating the Displacement Spectral Densities of the measured profiles in this study.

## 2.9. International Roughness Index (IRI)

Sayers and Karamihas (1998) provide information about measuring and interpreting road profiles. They also provide a very descriptive interpretation of the International Roughness Index (IRI). Almost every automated road profiling system includes software to calculate a statistic called the International Roughness index (IRI).

The IRI was the first widely used profile index where the analysis method was intended to work with different types of profilometers. IRI is defined as a property of the true profile and therefore it can be measured with any valid profilometer. The analysis equations were developed and tested to minimize the effects of some profilometer measurement parameters such as sample interval.

The IRI is calculated by simulating a quarter-car model, known as the Golden car, driving on the measured profile at 80 km/h. The absolute suspension travel of the quarter-car is added together and divided by the length of the input profile. The result of the absolute suspension travel divided by the length of the input profile produces the IRI value.

Let  $T$  be time it takes a vehicle to traverse a pavement section of length  $L$  at a constant speed of  $v = 22.22$  m/s. The IRI is defined by the average of the absolute value of  $\dot{z}_s(t)$  over time  $T = n\Delta t$ , ie. (Sun, 2001)

$$IRI = \frac{1}{L} \int_0^T |\dot{z}_s(t)| dt = \frac{1}{vn\Delta t} \sum_{i=0}^n |\dot{z}_s(t_i)| \Delta t = \frac{1}{vn} \sum_{i=0}^n |\dot{z}_s(t_i)|$$

The IRI summarizes the roughness qualities that impact vehicle response and is most appropriate when a roughness measure is desired that relates to: overall vehicle operating cost, overall ride quality, dynamic wheel loads and overall surface condition. The standard IRI values for different road surfaces are tabulated in Table 1.

Road Surface	IRI (m/km)
Superhighways	0.25 - 1.9
New pavements	1.45 – 3.3
Older pavements	2.2 – 5.75
Maintained unpaved roads	3.4 – 9.9
Damaged pavements	4 – 10.9
Rough unpaved roads	8 - 20

Table 1: IRI values for different roads.

Figure 18 shows IRI ranges represented by different classes of road.

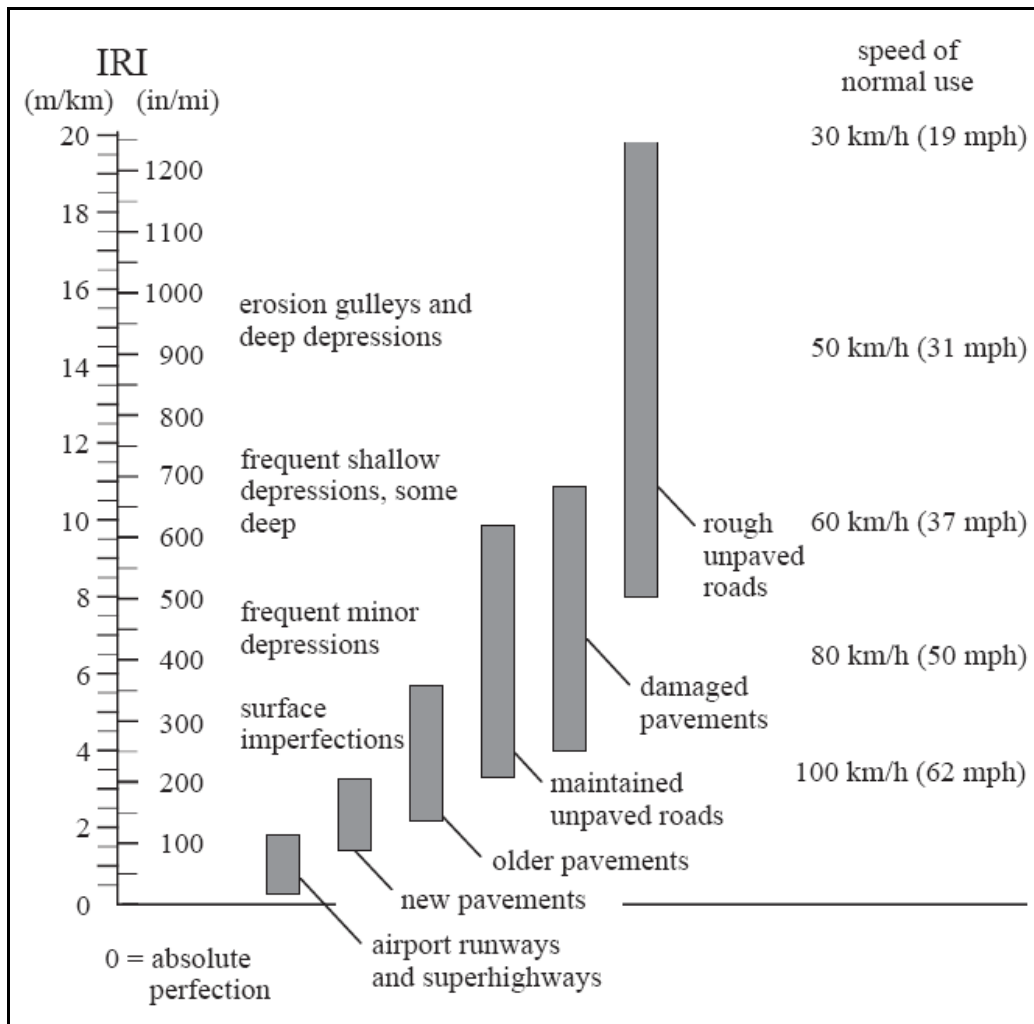


Figure 18: IRI ranges representing different classes of road (Sayers and Karamihas, 1998).

The Golden car quarter-car model used in calculating the IRI is just what its name implies: a model of one corner (or quarter) of a car as indicated in Figure 19. The model includes one tyre, represented with a vertical spring, the

mass of the axle supported by the tyre, a suspension spring and damper and the mass of the body supported by the suspension for that tyre. The quarter-car model was tuned to maximize correlation with response-type road roughness measuring systems. The Golden car parameters give the quarter-car a behaviour typical of most highway vehicles with one exception: the damping is higher than most cars. This keeps the IRI from “tuning in” to certain wavelengths and degrading correlation with other vehicles.

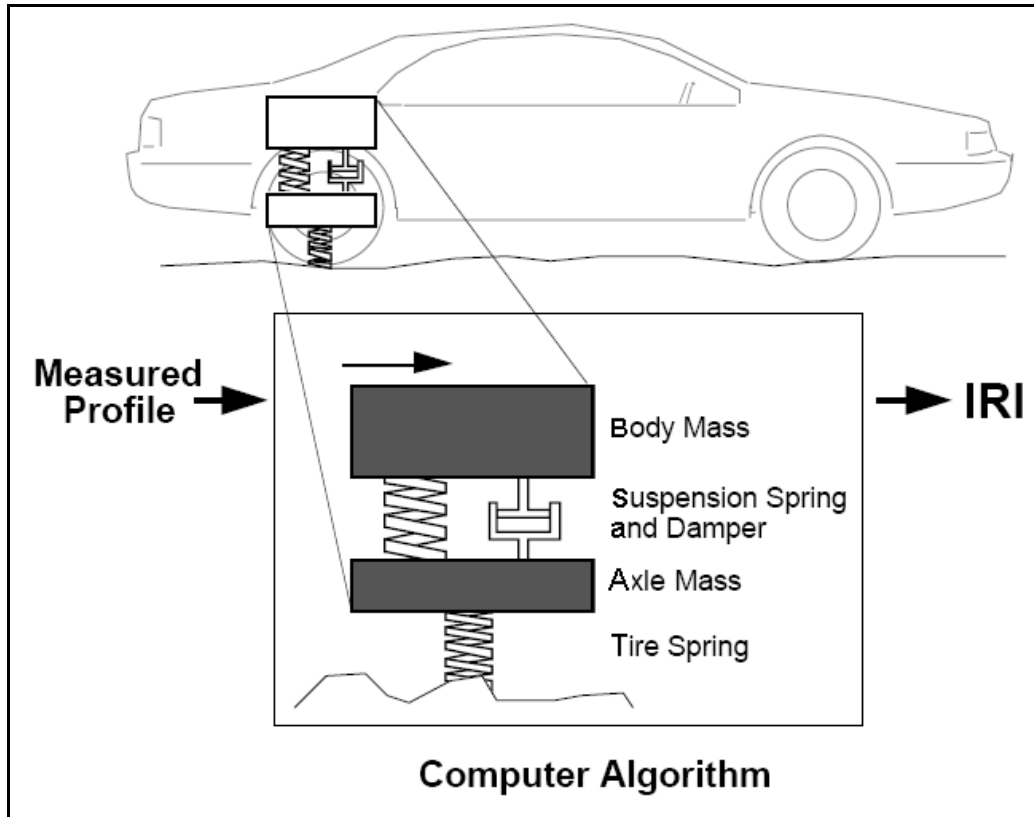


Figure 19: Golden car, IRI quarter-car model (Sayers and Karamihas, 1998).

## 2.10. Summary on literature survey

From the literature study the following conclusions were drawn and the proceedings of the study were consequently adapted.

The High Speed Profilometer, Inertial profilometer, Lightweight profilometer, Walking profilometer and Longitudinal Profilometer Analyser could not be used in our application since they only profile the longitudinal and transverse profiles in the wheel tracks of the vehicle used and a 2-D model of the road could be generated. The HSP was also designed to profile concrete roads and asphalt roads at high speeds. The HSP was also restrained by a lower operation speed limit of 12 km/h. In some instances this lower operating speed limit was a too high travelling speed for some of the off-road terrains

which were required to be profiled. Also the vehicle which the HSP is mounted is not suitable for some of the terrains.

The Rod and Level and the Dipstick methods may be used if a single line profile of the terrain were to be used in simulations but would be too time consuming to measure a 3-D profile of the terrain.

The use of 3-D tyre models in simulations are increasing and thus 3-D road profiles are required. In 3-D simulations the road is often modelled as separate left and right surfaces to reduce the number of elements in contact with the tyre, as it reduces the solver duration. The resolution of the Vehicle Terrain Measurement System is very high and not required due to the simulations programs not being able to process the amount of data and the higher resolution does not affect the vertical response of the model if a 3-D tyre model is used. Some tyre models are capable of handling complete 3-D contact. If more data is recorded than required every second or third data point may be used, thus one is still able to use very high resolution data. A higher resolution road profile may have an effect on the vertical response of the model if a point contact is used in the model. When a 3-D tyre model is used in a simulation the mesh size of the road profile used for the simulation should not be larger than half the contact patch of the tyre. Thus one is able to use a road profile with a mesh size smaller or equal to 100 mm in the direction of travel. The biggest problem with their system is the cost of the system and the system's capability is limited to the vehicle on which the system is mounted.

Photogrammetry and stereo techniques with aerial imagery is a possible option in profiling rough terrains. No literature was obtained where actual rough terrains were profiled with the use of Photogrammetry but it remains an option worth investigating for the profiling rough terrains.

Laser scanning platforms are very accurate systems but the accuracy is compromised by the Global Positioning System when the 3-D model is placed in a global coordinate system. These systems have colossal raw data bundles and require state of the art computers for effective data processing. The laser scanning platforms are highly-priced and way beyond the resources for this study. The Laser scanning platforms are widely available however the vertical height required in order to profile a 100 m section of a terrain may compromise the obtainable resolution of the profile.

The terrain is classified with the use of a Displacement Spectral Density of the terrain which is an effective method in determining the roughness of the terrain. Terrains are classified in eight different types of roads ranging from a class-A road, which is a very smooth road up to a class-H road, which is an extremely rough terrain and only intended with the use of an off-road vehicle. The IRI is also a valid method used in comparing profiles of different terrains as well as comparing the same terrain profile, profiled with different profilometers.

It is important to know the orientation of the profilometer when a terrain is profiled because the terrain is profiled relative to the profilometer. Most of the terrains used for testing by the University of Pretoria have a known horizontal reference with a fixed height around the terrain. The known horizontal reference is in the form of a level surface around each terrain. The constant reference simplifies the method used to obtain the orientation of the profilometers.

For the present study three profilometers are constructed with the known level reference in mind. The first profilometer is a mechanical profilometer on three wheels, each moving on the known level reference. The second profilometer profiles a terrain with the use of Photogrammetry and the third profilometer utilize a laser which is mounted in a gimball.

### 3. Test Equipment

In this paragraph the three profiling methods proposed in this study for obtaining profiles of rough terrains are described. The development, working principals, testing and calibration of suitable equipment is discussed. Individual tests were conducted on each method to validate the profile obtained.

It is required that the profilometers are capable of the following;

- Profile rough terrain (vertical displacements > 25 mm).
- The mesh size of the profiled road may not be larger than half the contact patch of the tyre. Thus the mesh size is required to be smaller or equal to 100 mm in the direction of travel for typical tyre sizes.
- Effective profiling with minimal resources required.
- Minimum profile width of 2.5 m.
- Profile terrain with vertical accuracy < 5 mm.
- Profilometer must be light weight and easily transported.
- The cost of the profilometer should be kept to a minimum.
- The profiling speed < 6km/h, a fast walking speed.

In the light of these requirements, three concepts have been chosen for further investigation and development namely:

1. A mechanical profiler using arms pivoted to a reference frame on one side with small wheels on the ends in contact with the ground, nicknamed the Can-Can machine (see paragraph 3.1).
2. Photogrammetry using a digital camera mounted on a tripod above the terrain (see paragraph 3.2).
3. A laser displacement scanner mounted in a gimball that is rotated by two stepper motors (see paragraph 3.3).

#### 3.1. *Can-Can Machine*

The Can-Can Machine is a mechanical measuring device which profiles a terrain by measuring angles. When you drag your hand over a surface, the surface may be smooth or rough; the movement of your fingers gives you a feel for the profile of the surface. If an obstacle is in the way, your fingers simply bend at the top knuckle and move over the obstacle. Another explanation could be if you are sitting on a wheeled office chair with your legs kept firm with your heels on the floor. When the chair is pulled backwards your heels will follow the profile of the floor by pivoting your legs at the knees. This is the principle behind the operation of the Can-Can Machine.

The Can-Can Machine is a light weight, right angle triangular structure with a wheel on each corner of the structure (see Figure 20). The two rear wheels are mounted 4.5 metres apart and the front wheel is used to steer the structure. The rear wheel track width of 4.5 meters facilitates the profilometer in utilizing the smooth and level zero reference surfaces on either side of the profiled terrain on the Gerotek suspension track. A 12 Volt wiper motor is mounted on the frame of the wheel and a chain is used to drive the wheel. A 5 amp adjustable voltage regulator (LM338K) is used to build a speed control to adjust the profiling speed. The speed control can adjust the speed from standing still to 1 km/h, a slow walking pace. Figure 21 shows the wiring diagram of the speed control. The speed of the profilometer is low to eliminate any dynamic effects of the profilometer.

A Crossbow tilt sensor is mounted on the rear beam and provides the orientation of the rear beam in both pitch and roll directions. The rear beam is designed for a maximum deflection of 3 mm at the centre of the beam with all the required equipment mounted on the beam.



**Figure 20: The Can-Can Machine on the Fatigue track at Gerotek.**

Thirty arms are mounted 100 mm apart on the rear beam of the structure and they follow the profile of the terrain (see Figure 22). The thirty arms allow the Can-Can Machine to profile a 3 meter wide section of the terrain. Each arm has a 30 mm nylon wheel at the one end which is in contact with the terrain. Nylon wheels are used since the nylon wheels were found to have a lower tendency to bounce on the terrain than rubber wheels.

The displacement at the tip of the arm is calculated by measuring the angle at the pivot point. The angles are measured with the use of high precision single turn potentiometers. The potentiometers are mounted inline with the pivot point of the arms. The arms and potentiometers are attached to one another with plastic tubing to compensate for some misalignment (see Figure 23). The arms are all bent with the same curve and at the same angle. This is done to



allow the wheels to move over a large obstacle without the arms coming into contact with the obstacle.

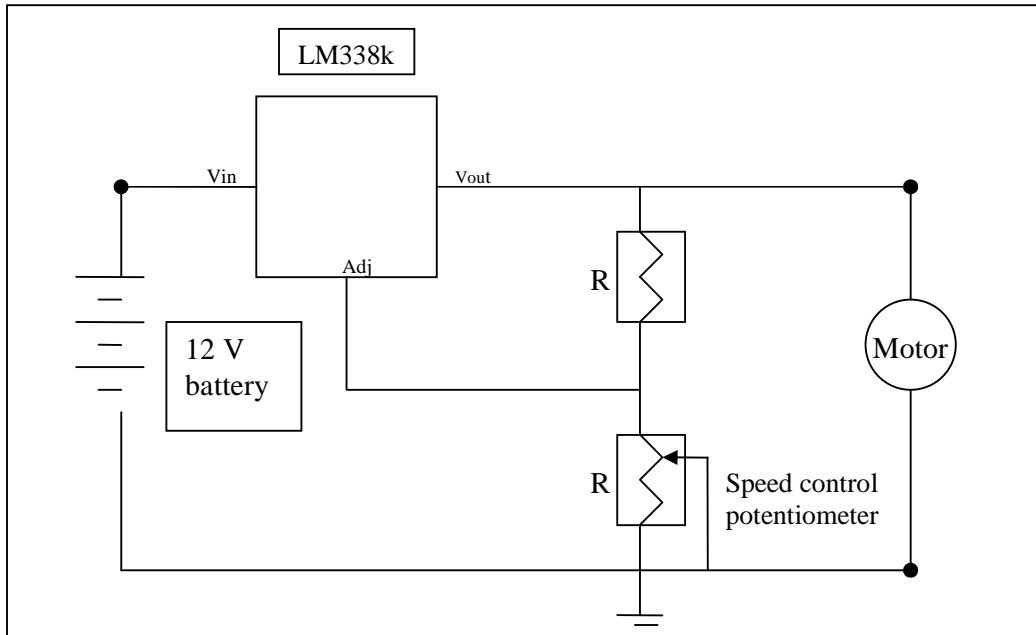


Figure 21: Wiring diagram of speed control for the Can-Can profilometer.

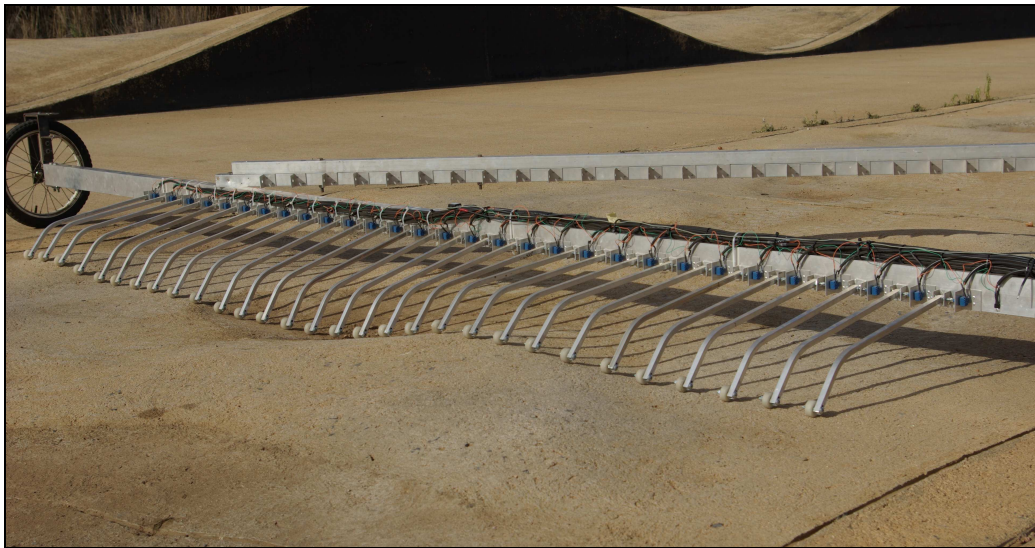


Figure 22: Thirty arms mounted on the rear beam of the Can-Can.

The potentiometers used on the Can-Can Machine are good quality Bourns 93R cermet track 10k $\Omega$  linear 16 mm, 2 Watt single turn potentiometers which have a 10% tolerance, 5% linearity and a temperature coefficient of 150. A LM 7805 5 Volt voltage regulator is used in supplying a regulated 5 Volts to all of the potentiometers. Figure 24 shows the wiring diagram of the LM 7805 which supplies a regulated 5 Volt to each potentiometer.

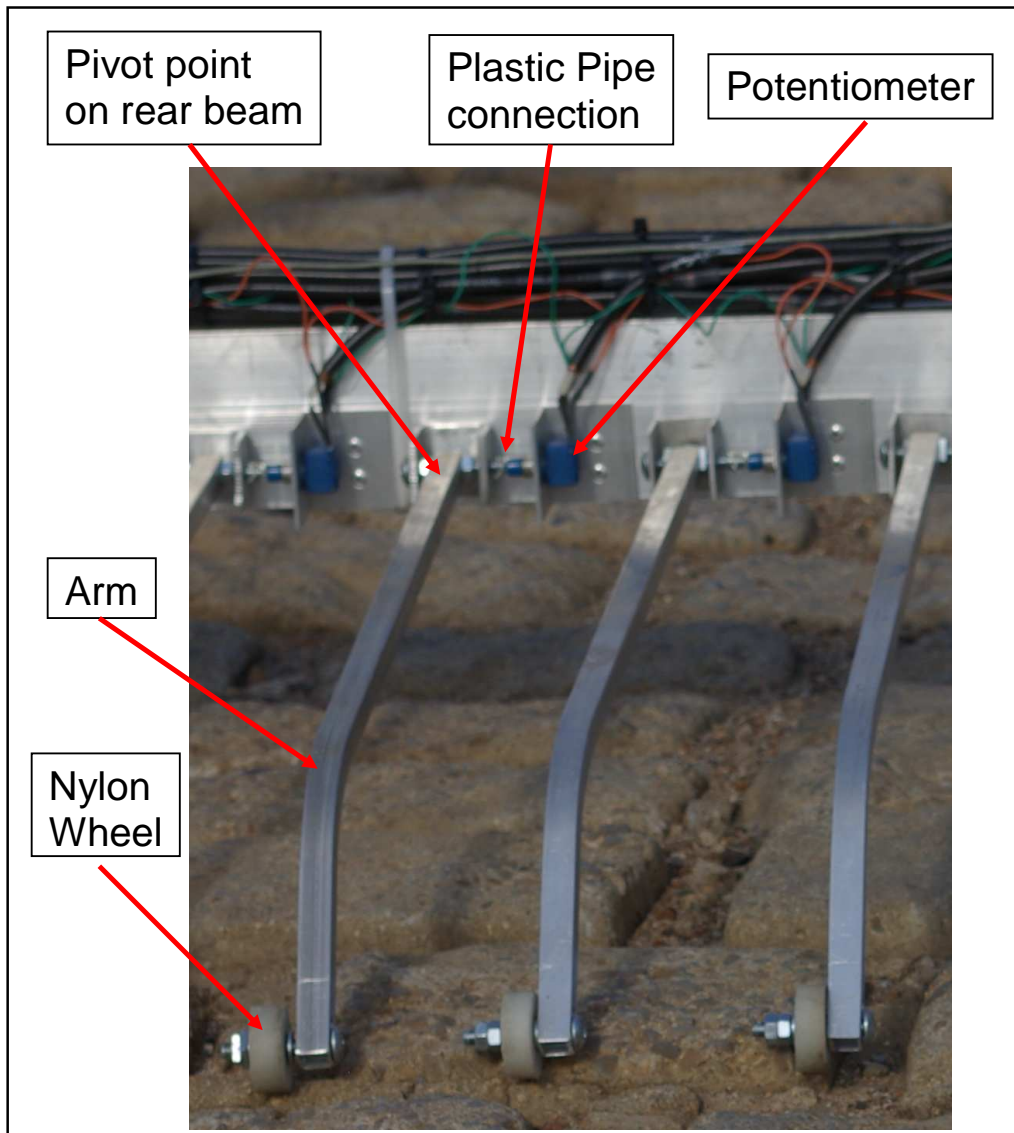


Figure 23: Close up of the arms and the potentiometers.

Although high precision linear potentiometers are used, as a check every fifth potentiometer is calibrated to determine the voltage output in relation to the rotation of the potentiometer due to the arm movement, the average of the calibrated potentiometers are used as the calibration factor for all the potentiometers. This is done because all of the potentiometers were purchased from the same supplier and were from the same production consignment. The calibration is done with the use of a dividing head, which is generally used on a milling machine. The chuck of the dividing head rotates once for every 40 revolutions of its side wheel. The rotating end of the potentiometer is placed in the chuck, the base of the potentiometer is kept static and the chuck is rotated. The voltage output of the potentiometer is measured for every two revolutions of the side wheel (every  $9^\circ$ ) (see Figure 25).

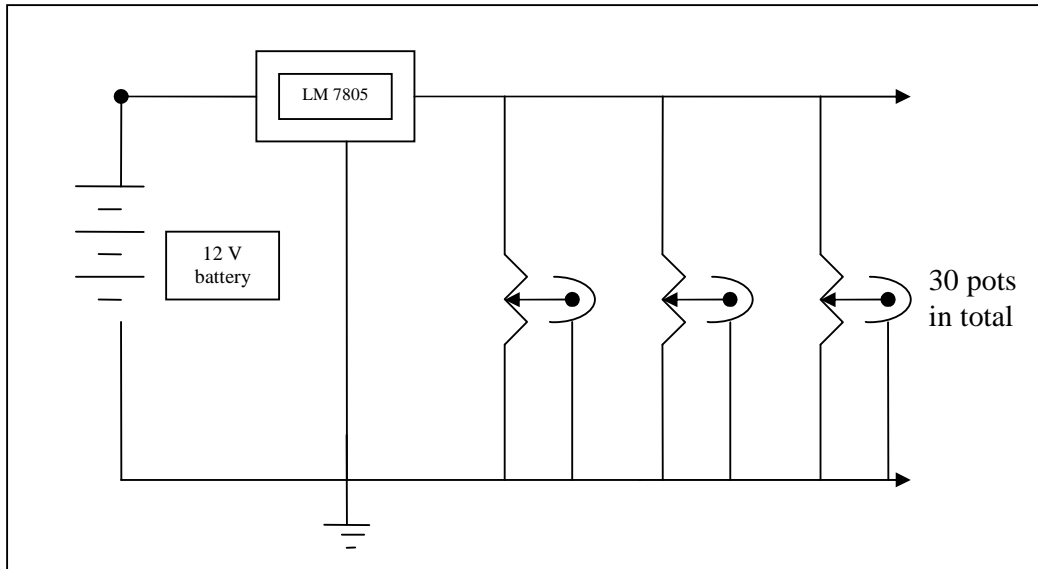


Figure 24: 5 Volt power supply for potentiometers.

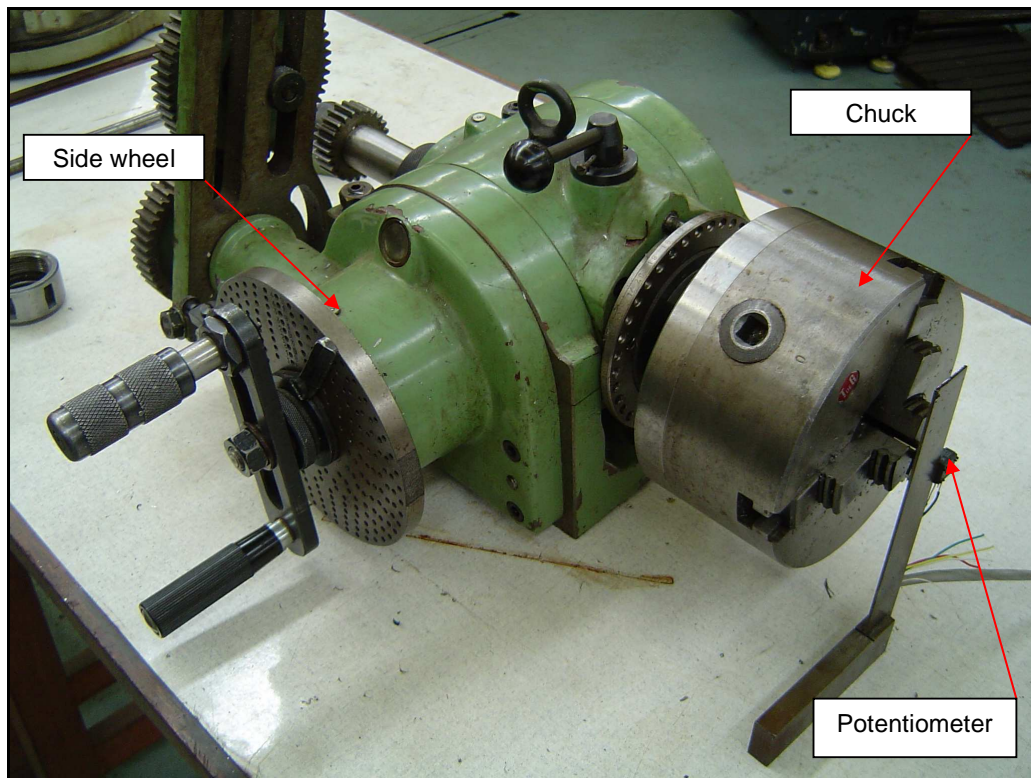


Figure 25: Calibration of potentiometers with the use of a dividing head.

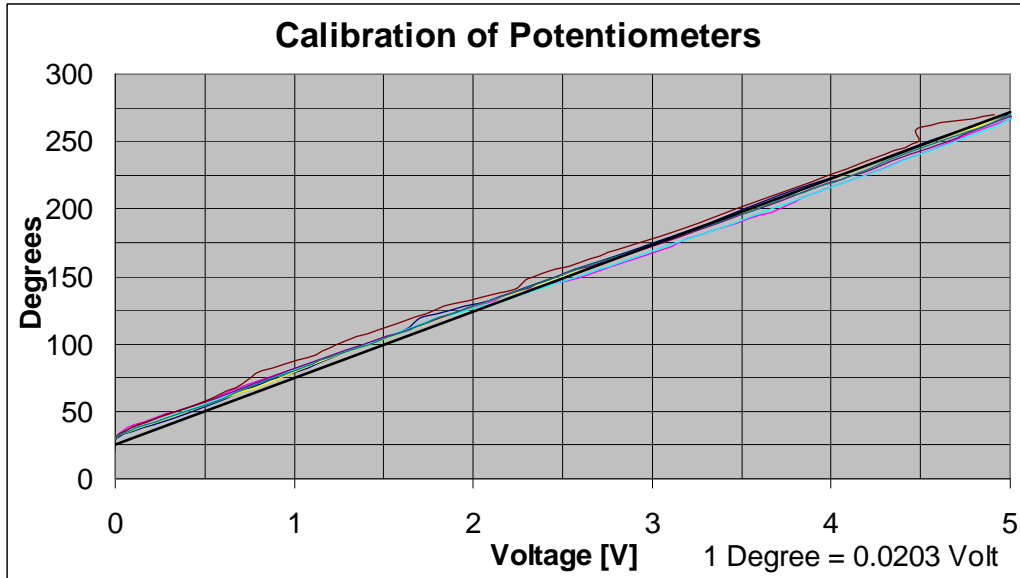


Figure 26: Calibration graph of potentiometers.

The degrees and measured voltage output are plotted to determine the voltage calibration value (see Figure 26). The gradient of the line in the figure is equal to the calibration value of the potentiometers, which is  $49.156^\circ/\text{Volt}$ . This indicates that for every  $49.15$  degrees of rotation the output voltage of the potentiometer changes with one volt. The calibration graph also indicates that the potentiometers are linear.

A 5 volt, 12-bit resolution ( $4096$  or  $2^{12}$  steps), Analogue to Digital converter is used to convert the analogue values to digital format which is in turn recorded on a data logging computer. The resolution of the converter is determined by dividing the voltage amplitude of the converter by the converter bit size minus 1.

$$\frac{\text{Voltage\_amplitude}}{(\text{bit\_size} - 1)} = \frac{(-5 \rightarrow 5\text{Volts})}{(2^{12} - 1)}$$

$$= \frac{10}{4095}$$

$$= 0.00244\text{V}$$

Thus the resolution of the potentiometers is calculated by multiplying the potentiometer calibration value with the converter resolution, which results in the following potentiometer resolution;

$$49.156^\circ / \text{V} * 0.00244\text{V} = 0.12^\circ$$

The length of the arms,  $L$ , from the contact point on the terrain to the pivot point is  $470$  mm. With the angle resolution,  $\theta$ , of the potentiometers known it is

possible to calculate the obtainable resolution of the concept in the vertical direction,  $z$ .

$$\begin{aligned} z &= L \sin \theta \\ &= 470 \sin 0.12^\circ \\ &= 0.98 \text{ mm} \end{aligned}$$

This indicates that the combination of the potentiometers and the analogue to digital converter has a resolution of 0.98 mm.

As the profilometer moves forward the tips of the arms move over the terrain causing the arm to pivot on the potentiometer. This arc motion at the tip of the arm causes an adjustment on the potentiometer equal to  $\theta$  degrees (see Figure 27).

The potentiometer gives a different voltage output as the angle  $\theta$  varies and is recorded by the converter. The variation in the potentiometer voltage output is used to calculate  $\theta$ , which in turn enables the computation of the point ( $X$ ,  $Y$ ) as follows:

$$\begin{aligned} \theta_0 &= \sin^{-1} \left( \frac{197}{L} \right) \\ \beta &= \theta + \theta_0 \\ X &= -L \cos \beta \\ Y &= -L \sin \beta + 197 (\text{ground\_reference}) \end{aligned}$$

The horizontal ground reference,  $\theta_0$ , is determined with the wheels at the end of the arms horizontally in line with the pivot point after which the zero reference,  $\theta_z$ , is determined. The zero reference is the constant height of 197 mm at which the potentiometers are mounted on the rear beam from the ground. With this array of points calculated, the programme written in Matlab is able to plot the terrain in three dimensions as required. In order to keep  $X$  to a minimum, the rear beam is mounted as low as possible with sufficient clearance for the rough terrain to pass below the beam. A Matlab programme is written to plot the recorded data and can be used to plot any recorded section of a terrain.

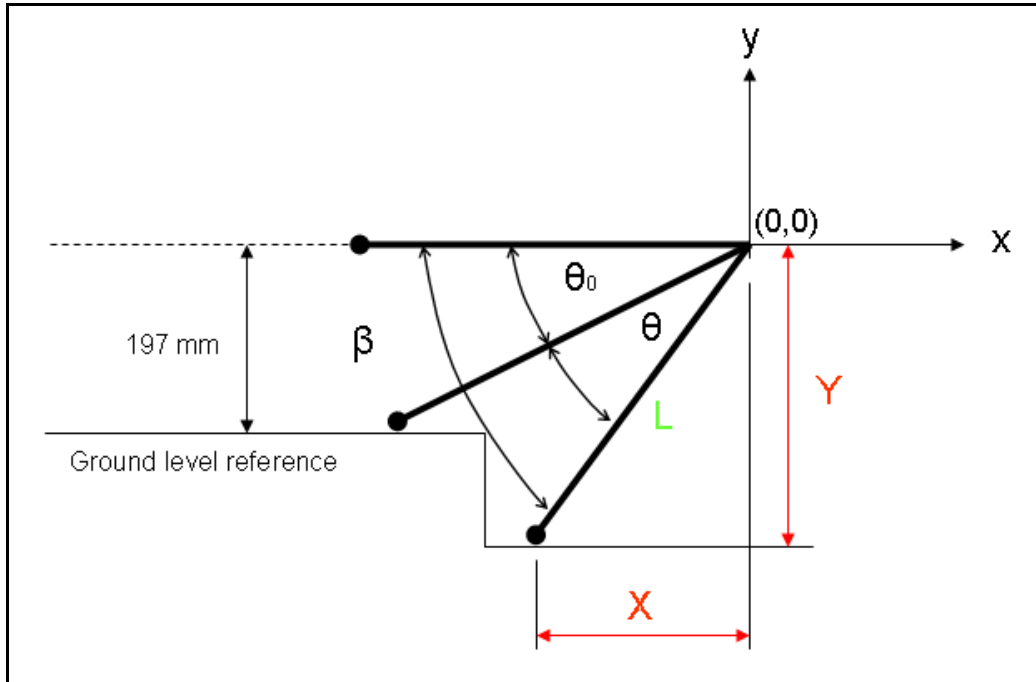


**Figure 27: Description of the arm movement.**

To measure the global  $X$  position of the pivot point, a digital encoder is designed and built in-house (see Figure 28). The encoder is mounted on the driving wheel and digitally triggers the data acquisition system with the use of two slotted opto-couplers. Data from the potentiometers and the tilt sensor are therefore recorded at constant horizontal distance intervals. The two slotted opto-couplers are mounted at an offset which enables the system to detect whether the Can-Can is moving forwards, backwards or standing still. The encoder has 120 triggers per revolution of the wheel, which gives a trigger every 10.18 mm of horizontal movement. The use of the encoder enables the data acquisition system to operate according to the operating speed of the Can-Can Machine, thus the system samples faster if the Can-Can Machine is operating at a faster speed and slower if the Can-Can is moving slowly. The encoder has two continuous potentiometers which rotate with the encoder without slip. The output of the continuous potentiometers indicates whether the opto-couplers are operating correctly.

When the encoder triggers, the data acquisition system samples 10 points on each channel in quick succession and saves the average of the 10 points. This average filters the electrical noise from the data and provides a smoother, more accurate profile.

The terrains profiled on the Suspension track at the Gerotek Test Facilities have level and smooth concrete sections on both sides of the terrain which provide a fixed reference for the profilometer.

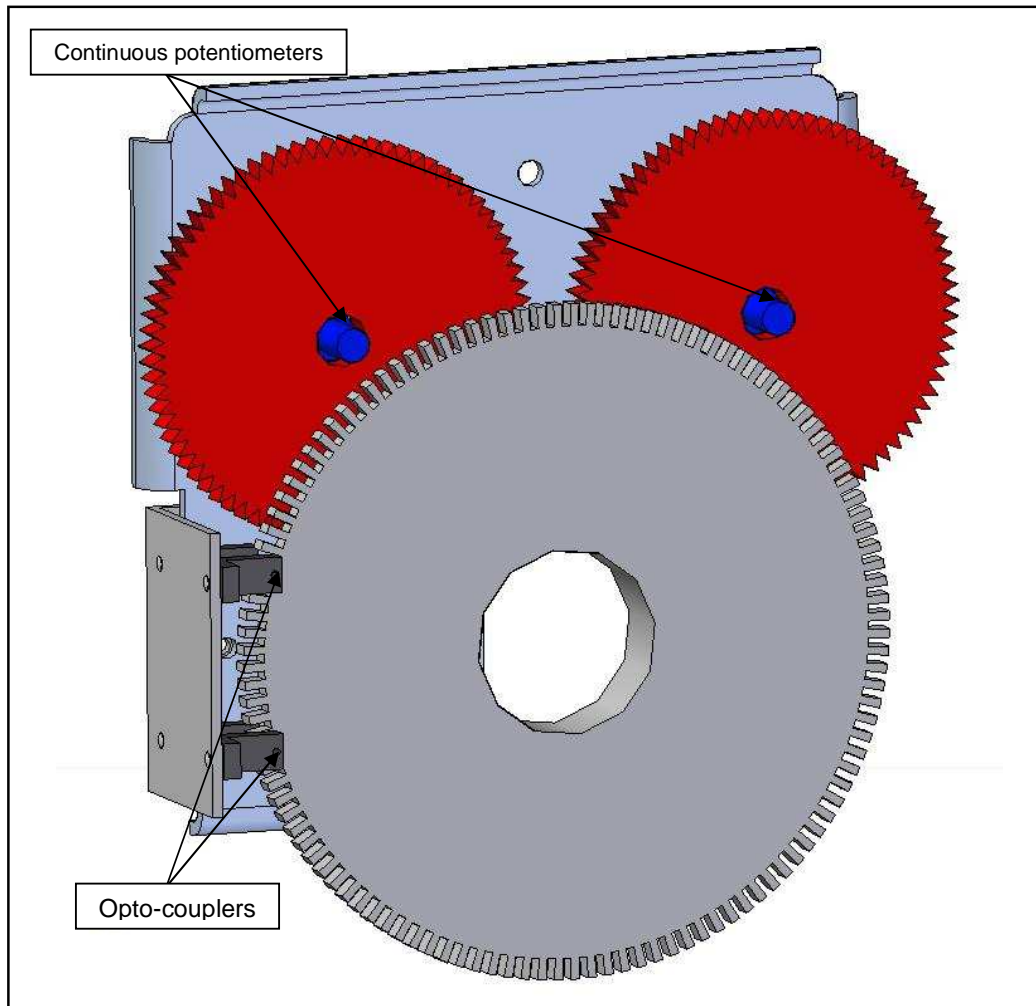


**Figure 28: Encoder used to trigger data acquisition system.**

The other terrains profiled with the Can-Can Machine require fixed references due to the fact that the whole structure of the profilometer moves over the rough terrain. The fixed reference is obtained with the use of a tilt sensor, surveying equipment and two straight beams on which two of the three wheels move.

A Crossbow CXTA02 tilt sensor is mounted in the middle of the rear beam and is used to determine the orientation of the Can-Can Machine in both pitch and roll. The certificate of conformance can be seen in Appendix A. This type of tilt sensor is based on an accelerometer and therefore calculates the tilt angle based on the gravity vector. It is therefore only accurate at low frequencies and the frequency range in which it gives acceptable accuracy had to be determined. Thus tests were conducted to determine the maximum frequency at which the tilt sensor can operate. The tilt sensor was mounted at 43 degrees on an actuator as shown in Figure 29.

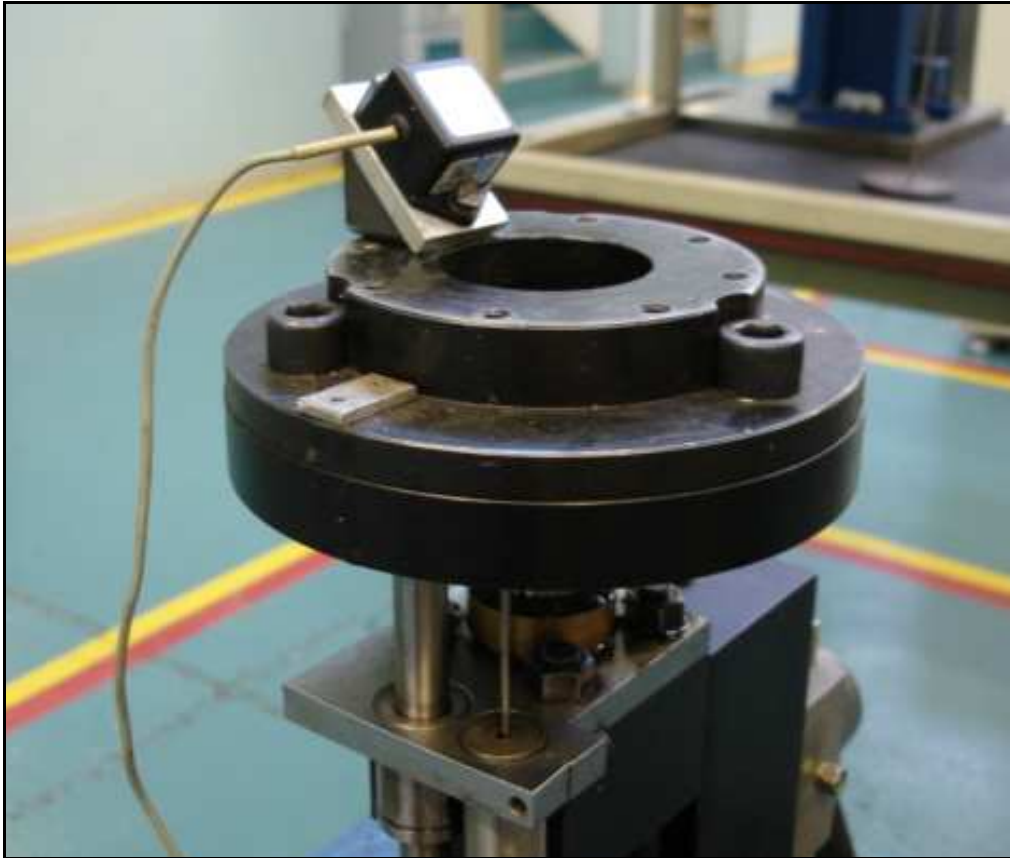


**Figure 29: Crossbow tilt sensor mounted on an actuator at 43 degrees.**

A 0 to 1 Volt random signal with a frequency content from 0 to 4 Hz was generated to excite the actuator over a period of 600 seconds. The response of the tilt sensor to the random input can be seen in Figure 30. The top graph in Figure 30 shows the input signal to the actuator. The middle graph shows the measured response from the tilt sensor and indicates significant noise of up to  $4^\circ$  superimposed on the true  $43^\circ$  orientation. The bottom graph shows the Fast Fourier Transform (FFT) of the tilt sensor's response.

It can be seen from the FFT graph in Figure 30 that the tilt sensor has a natural frequency between 2 and 3 Hz. The response of the tilt sensor was filtered with a 0.1 Hz low-pass RC filter. A 0.1 Hz low-pass RC filter was used due to the fact that the Can-Can Machine moves very slowly and the assumption was made that frequencies higher than 1 Hz will not be generated when the Can-Can Machine is profiling a terrain. The wiring diagram of the simple passive RC filter is shown in Figure 31.



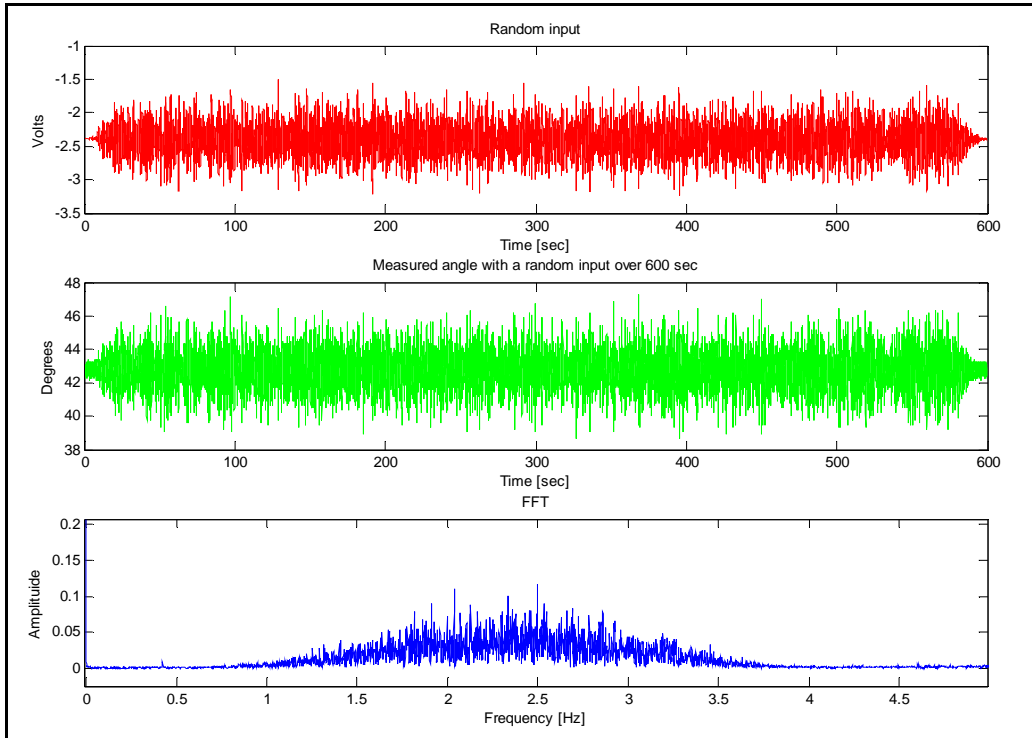


**Figure 30: Response of tilt sensor to a random input.**

The time constant of the filter,  $\tau$ , is calculated as follows;

$$\tau = RC$$

with

$$R = 1M\Omega$$

$$C = 1.5\mu F$$

thus

$$\tau = (1e6)(1.5e-6)$$

$$= 1.5 \text{ sec}$$

The cut-off frequency,  $f_c$ , of the RC filter is calculated as follows;

$$f_c = \frac{1}{2\pi RC}$$

$$= 0.106 \text{ Hz}$$

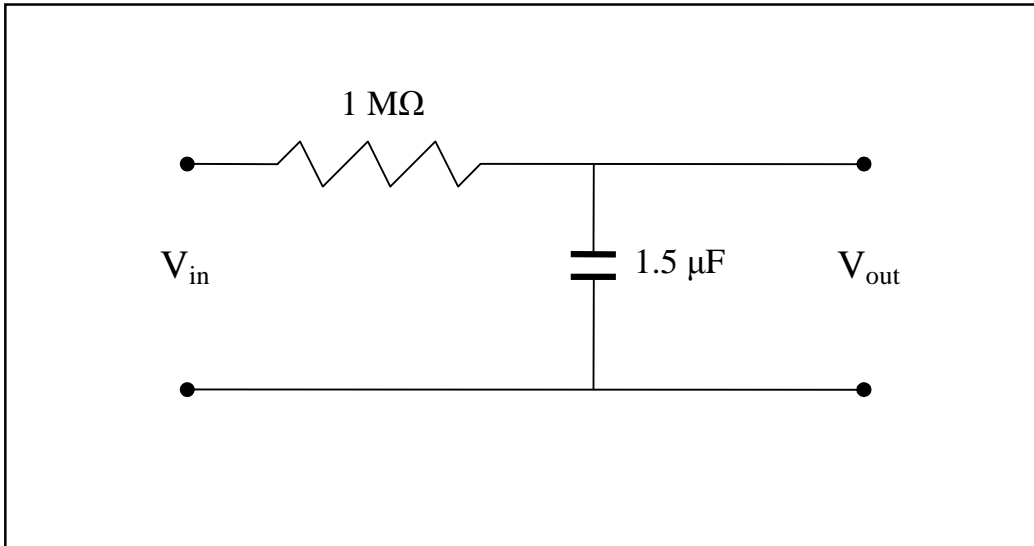


**Figure 31: 0.1 Hz RC Filter.**

The top graph in Figure 32 shows the FFT of the tilt sensor's response and the applied low-pass RC filter. The bottom graph shows the difference between the raw data and the filtered data from the tilt sensor's response. It is clear that the low-pass RC filter has a dramatic improvement on the measuring capability of the tilt sensor and thus the decision is made that the tilt sensor is capable of providing steady measurements for determining the orientation of the Can-Can Machine when profiling a terrain.

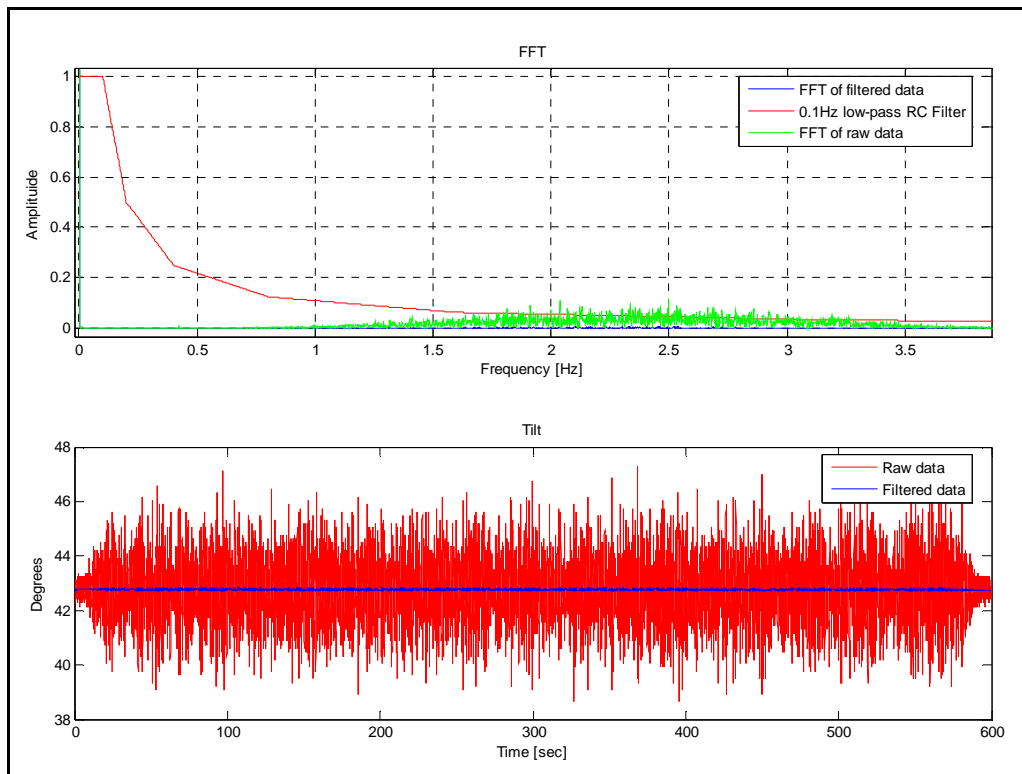


**Figure 32: 0.1 Hz Low-pass filtered response of tilt sensor to a random input.**

### 3.1.1. Test sections for Can-Can Machine

To verify correct operation and accuracy, the Can-Can Machine is tested in three different ways. The first method is used to test and investigate the accuracy of the arm movement. The profilometer was used to profile a 55 mm flat-top bump on a flat surface. The actual profile of the bump and the profile from the Can-Can Machine are shown in Figure 33.

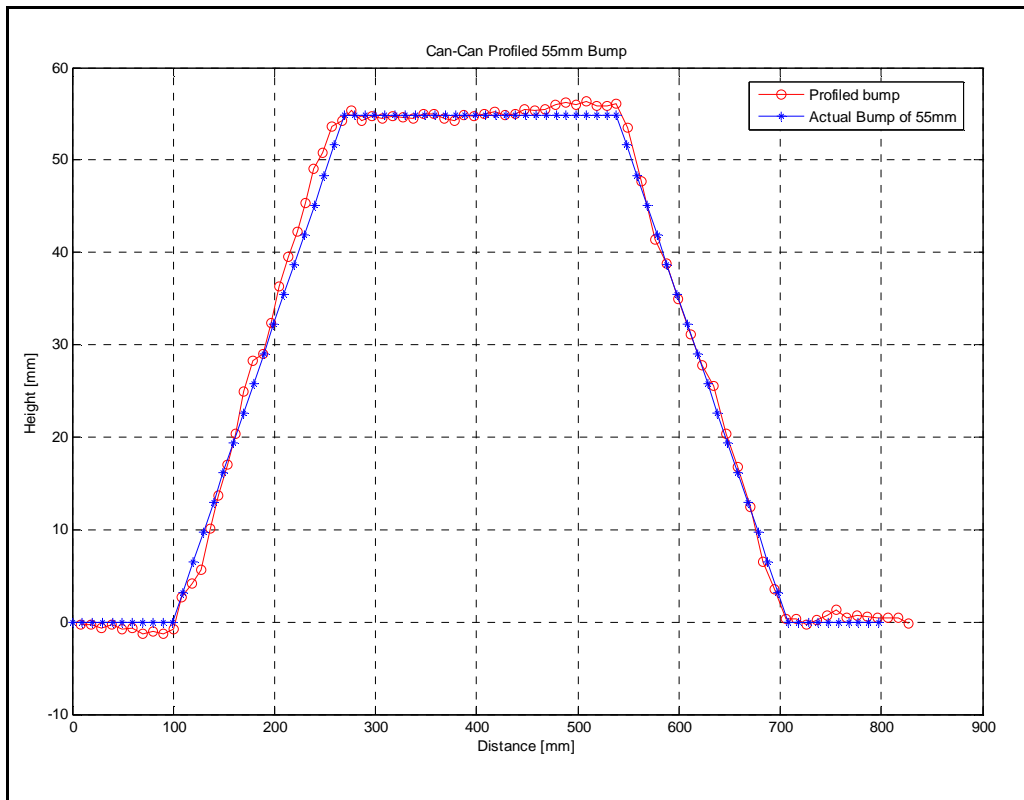


**Figure 33: 55 mm flat-top bump profiled with Can-Can Machine.**

The blue line in the figure is the actual profile of the bump and the red line is the bump profiled with the Can-Can Machine. The RMS value of the profile is 36.2 mm and the RMS value of the actual bump is 37.7 mm. The Root Mean Square Error (RMSE) represents the difference between the actual profile of the bump and the Can-Can profiled bump. The RMSE is given by the following formula:

$$RMSE = \sqrt{\frac{\sum_{i=1}^n (y_{i-actual} - y_{i-Can-Can})^2}{n-1}}$$

Where:

- $y$  is the error in the vertical direction of the profile
- $n$  is the number of points in the profile.

The RMSE in the vertical direction is calculated at 2.73 mm. The difference in the profiles at the top of the bump is due to the small wheels at the end of the arms, which have a diameter of 30 mm. This error may be decreased with the use of even smaller wheels at the tips of the arms which is used to follow the profile of the terrain. Smaller wheels are not used simply because if even smaller wheels are used more noise will be present in the profile. Another contributing factor in not using smaller wheels on the profiling arms is that the wheels on the arms of the profilometer are smaller than the actual vehicle's wheels by a factor of 25 and the high frequencies measured by the smaller wheels will not have an effect on the response of the vehicle in the simulations. The corners at the top of the actual bump have a small radius and can be seen if the actual bump is plotted with a finer resolution.

The second test performed on the Can-Can Machine is profiling a flat concrete surface when one of the profilometer's wheels is moving over a 105 mm flat-top bump. The purpose of this test is to determine if the tilt sensors can be used to successfully eliminate the effects of roll and pitch of the main beam if the three wheels of the Can-Can Machine move over rough obstacles.

The measured profile is adjusted with the use of the orientation of the profilometer as measured with the tilt sensor. The top graph of Figure 34 shows the profile with the effect of the orientation of the Can-Can Machine added to the measured profile. The bottom graph shows the profile of the flat measure concrete surface without the orientation of the profilometer added. It can be seen in the top graph of Figure 34 that the concrete surface is flat but not exactly horizontal, which is indeed the case with the surface used for this test. Figure 35 shows the difference in the two profiles obtained in Figure 34 and illustrates the importance of the addition of the orientation of the profilometer to the measured profile.

The difference in the profiles increases to the one side because only the left wheel of the Can-Can Machine moved over the 105 mm flat-top bump. It is clear that even with the addition of the tilt sensor the profile of the flat surface is still not exactly flat. The RMSE calculated from a zero reference was 17.87 mm. Figure 36 shows the tilt sensor data added to the measured profile. It can be seen that when the profilometer moves too fast over a big obstacle the tilt sensor does not stabilize. This is due to the 0.1 Hz low-pass RC filter applied to the tilt sensor data which has a time constant of 1.5 seconds. The black line in Figure 36 indicates that the tilt sensor did not stabilize and did not profile a flat top bump. In this case the tilt sensor should be a mirror image of the blue line which is the raw profile. This can be corrected by profiling at a lower speed when the profilometer needs to move over large obstacles, which in turn will also decrease the RMSE.

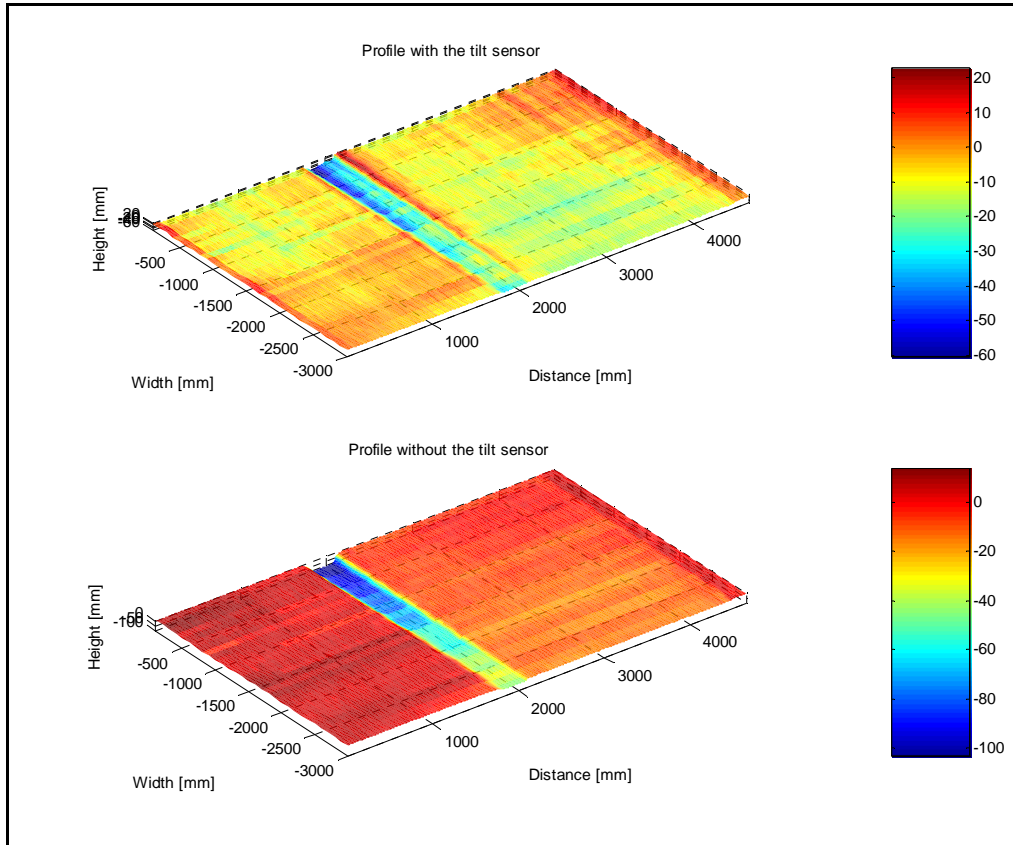


Figure 34: Profile of flat concrete surface.

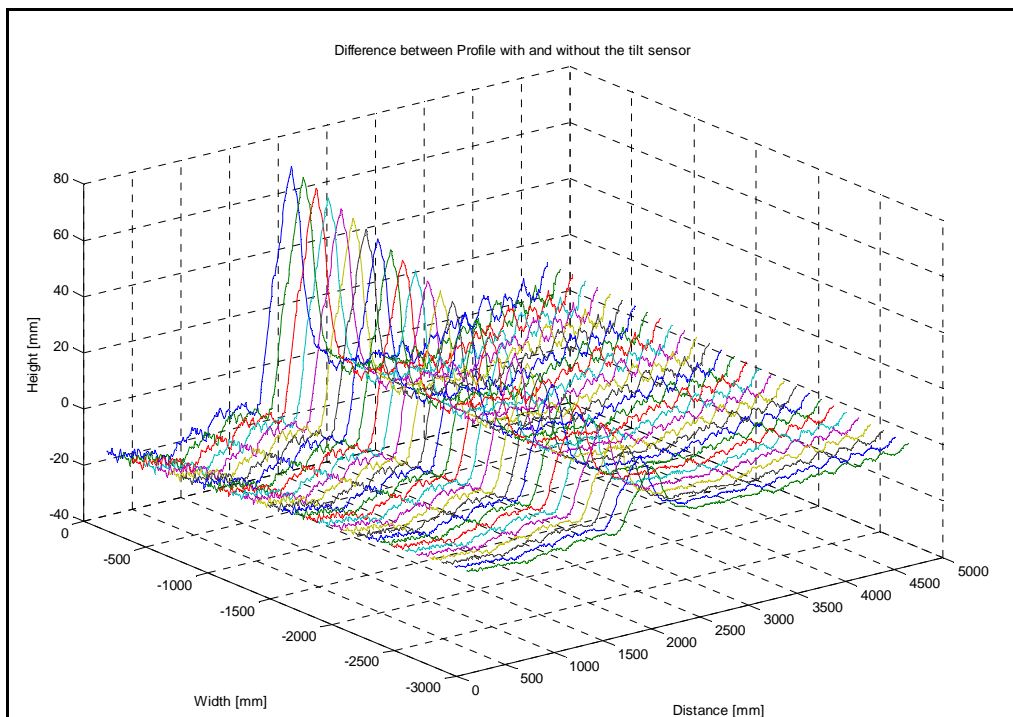
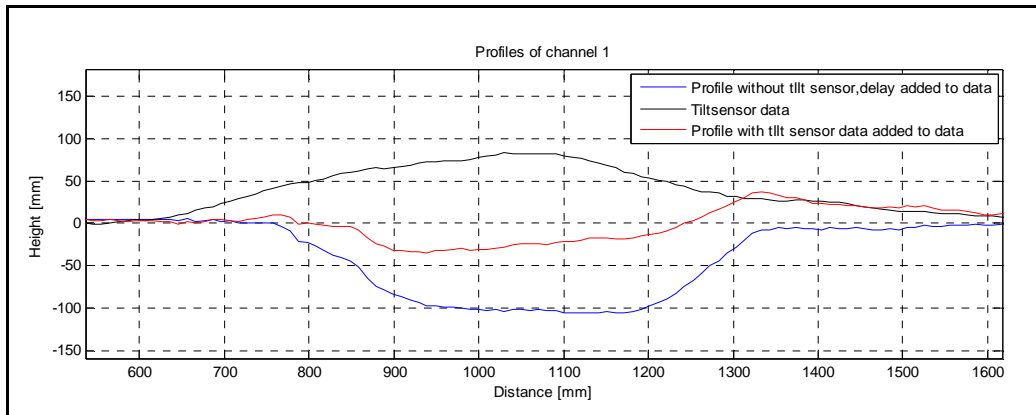


Figure 35: Difference in the profile of the flat concrete surface with and without the orientation of the profilometer.



**Figure 36: Profile of channel 1 for flat test section with Can-Can Machine.**

The third test conducted on the Can-Can Machine is a test that assesses the profile of test bumps profiled with the wheels of the profilometer also moving slowly over obstacles. Figure 37 shows the actual test section in which the Can-Can Machine profiled from left to right. Figure 38 shows the profiled test section. The top figure indicates the profile corrected using the tilt sensor data while the bottom figure indicates the uncorrected profile. The test section layout is as follows, the profilometer profiles a flat section with the left wheel of the profilometer moving over a 105 mm flat-top bump, and then a 55 mm flat-top bump is profiled without the profilometer moving over any obstacle. After the 55 mm bump is profiled the profilometer's left wheel moves over a 105 mm flat-top bump whilst profiling a 55 mm flat-top bump. Excellent results are achieved with the Can-Can Machine moving slowly over the obstacles in this test.

Figure 39 shows the different profiles of channel 1. This channel profiled the two 105 mm flat-top bumps just after the left wheel of the profilometer moved over them. The black line in Figure 39 is the tilt sensor data and it is clear that the slower profiling speed produces an accurate profile of the profiled terrain due to the fact that the tilt sensor data resembles the flat-top bump. The error in the profiled terrain is no more than 10%.

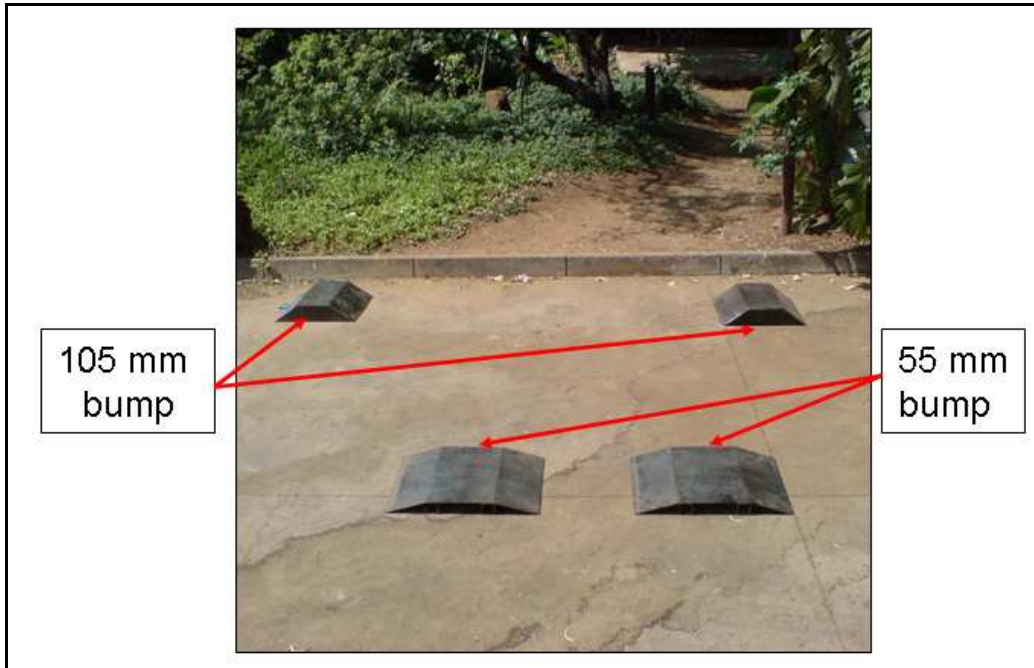


Figure 37: Final test section for Can-Can Machine.

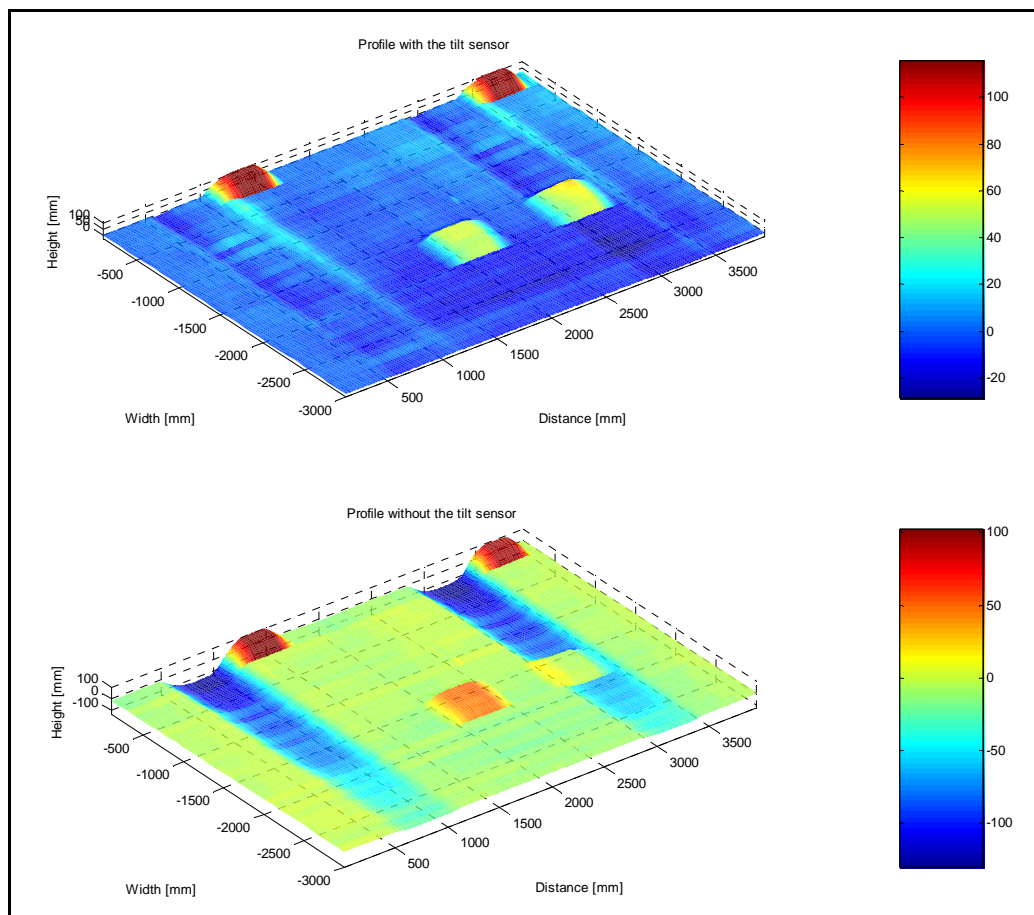
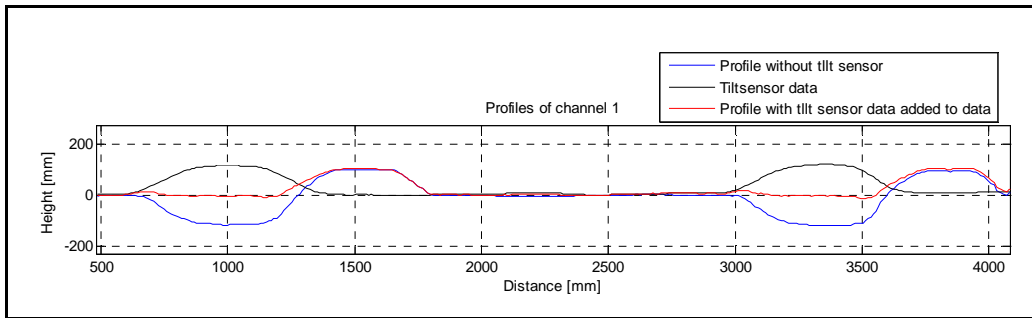


Figure 38: Profile of final test section for Can-Can Machine.



**Figure 39: Profiles from channel 1 for final test section with Can-Can Machine.**

The results obtained from the third test indicate that the Can-Can Machine is an accurate rough road profilometer which is not resource intensive and is capable of profiling any road surface. If very rough terrain is profiled the most accurate profile will be obtained by profiling the terrain as slowly as possible. The overall accuracy of the Can-Can Machine was found to be in the order of 5 mm (or less than 10% compared to the exact profile) when the profilometer moved over large obstacles.

### **3.2. Photogrammetric Profiling**

Photogrammetric profiling basically consist of taking overlapping photographs of the terrain from a suitable height, perpendicular to the terrain, using a calibrated camera. Targets on the terrain with accurately known coordinates are included in the photographs and are used for orientation and absolute reference. This technique is regularly employed for generating contour maps from aerial photographs. The question to be answered here is whether it could be used to measure much smaller profiles using a camera mounted much closer to the terrain.

The photogrammetry and mapping for the present study were implemented thanks to CAD MAPPING cc. Paragraph 3.2.1 to 3.2.5 describe the procedure followed by CAD MAPPING cc in obtaining the profile captured on the photographs. Paragraph 3.2.6 describes the test section employed to validate the use of photogrammetry to capture the profile of a rough road at such a low vertical height from the ground.

#### **3.2.1. Camera calibration**

An in-house camera calibration was done with the use of the calibration grid as seen in Figure 40. The calibration grid is a pattern of dots specifically designed for the calibration software. Each position on the grid is assigned a calibration value to determine the lens distortions, focal length and size of the



image (see attached calibration certificate in Appendix A). Camera calibration is a method for accurately determining values for a camera's parameters. Once a camera is calibrated, it will provide accurate measurements necessary for photogrammetry.

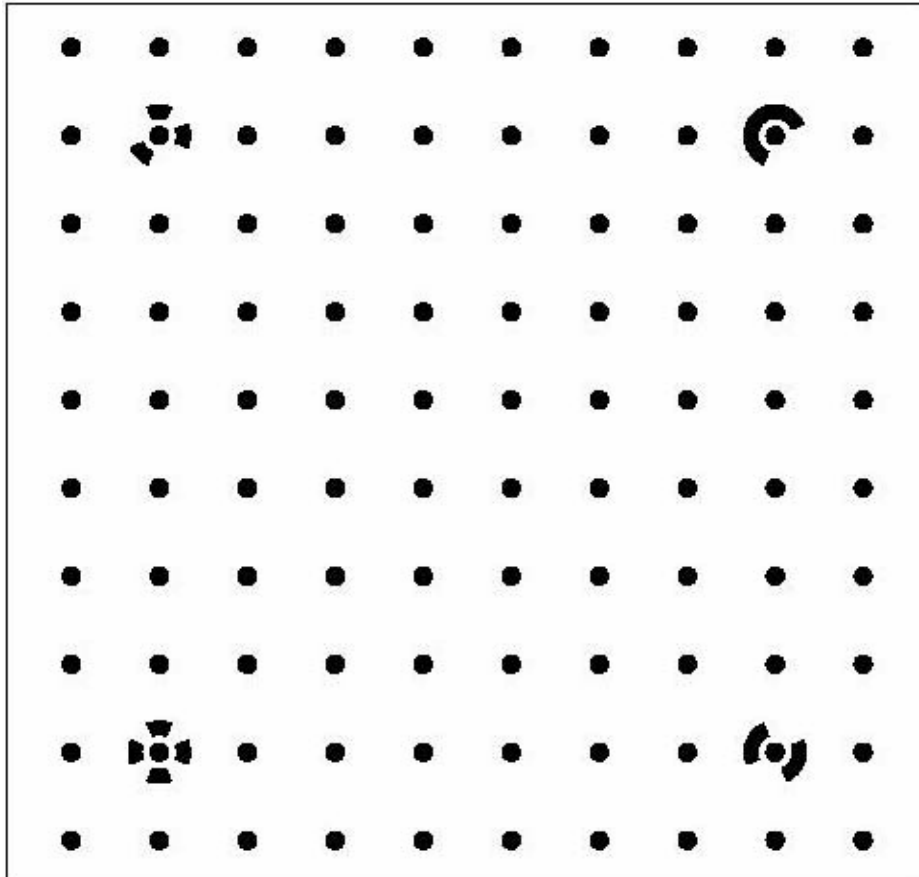


Figure 40: Calibration grid used for camera calibration.

### 3.2.2. Ground control

Pre-determined control points were marked with the use of targets along the terrain to be mapped and surveyed using a Total Station provided by the Topographical Department of The University of Pretoria and Pro Mapping cc (see Figure 41). Coordinates in a local system were obtained. A Total Station was used because the DGPS could only provide an accuracy of 12 mm on the position of the points surveyed, as where the Total Station was able to obtain a 3 mm accuracy. This accuracy was required to obtain exploitable results with the use of photogrammetry and gave an overall accuracy of 2 mm to 5 mm on the profile.



Figure 41: Ground control points surveyed using a Total Station.

### 3.2.3. Mapping

After the camera was calibrated and the control points were surveyed, photographs of the test section were captured with a standard off-the-shelf 5 mega pixel Sony Cyber Shot Digital camera. The lens of the digital camera was a Carl Zeiss lens with 3 x optical zoom which is equivalent to a 35 mm photography lens. For the test section the camera was placed in a custom build cradle as shown in Figure 42. The cradle was suspended 2 m above the ground between two vehicles with the use of a rope and pulley system. The imagery was subjected to further analysis using a digital photogrammetric workstation (see Figure 43).

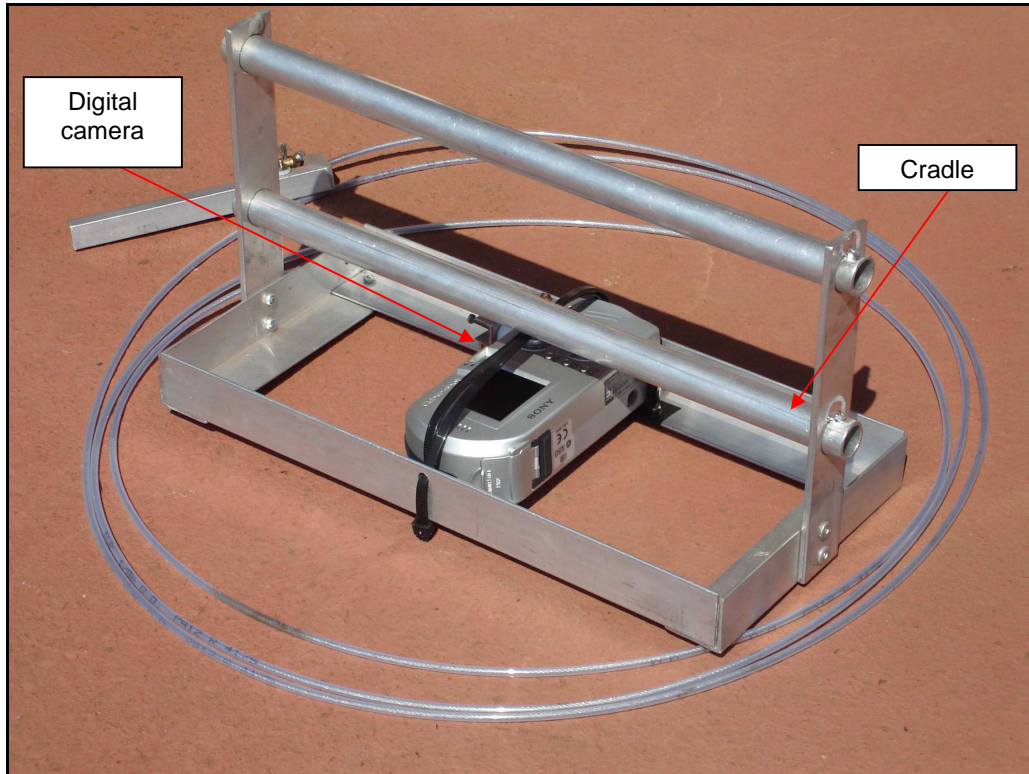


Figure 42: Cradle used for photogrammetry test section.



Figure 43: Digital photogrammetric workstation.

### 3.2.4. Triangulation inner orientation

An inner orientation was measured by observing the corners of each image as fiducial marks. The reference values for the physical position of the fiducial marks were obtained from the calibration certificate.

### 3.2.5. Aerial Triangulation

Aerial triangulation is a combined procedure used to determine the transformation from image coordinates to model and then ground coordinates. The routine enables users to observe Photo Ground Control (PGC) points and relative points, which were referred to as Von Gruber positions, in the stereo pairs along the entire strip (see Figure 44). These measurements were then used to determine perspective centre coordinates and exterior orientation angles. The observations can be used in a Bundle Block adjustment. The results determined by the Bundle Block can then be used in the absolute orientation of the stereo pairs.

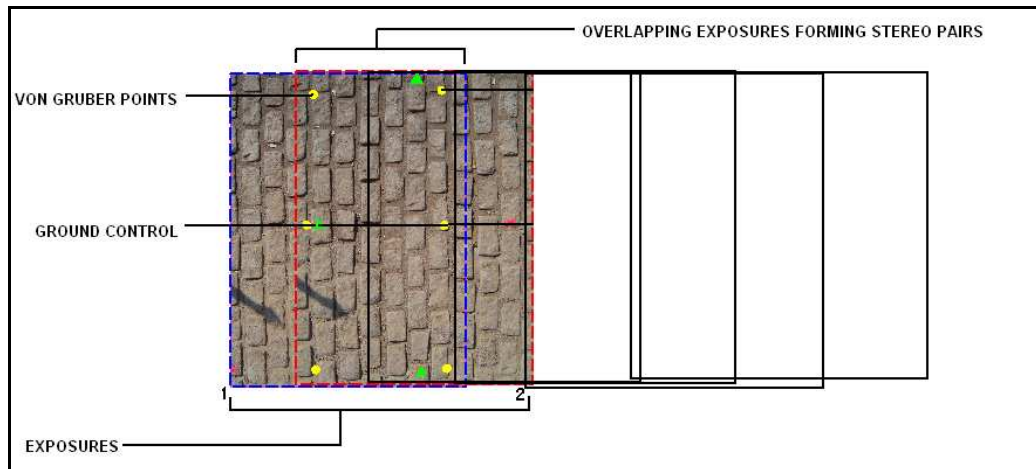


Figure 44: Stereo pairs, von Gruber points and ground control.

Break lines are read to determine the Triangle Network (TIN). The triangles provide three-dimensional information for surface creation and modelling. An example of the break lines and triangles are shown in Figure 45.

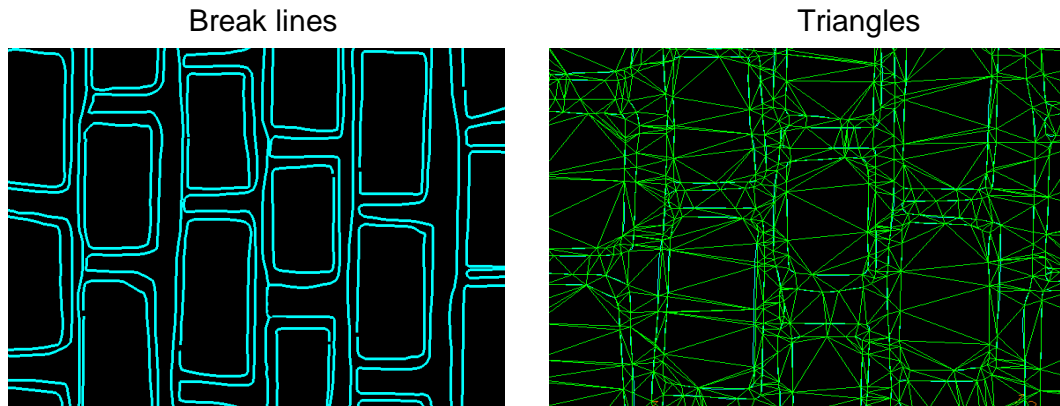


Figure 45 (a) and (b): Example of break lines and triangles.

### 3.2.6. Test section for photogrammetry

To determine if photogrammetry could be used for profiling obstacles at a close range an indicative experiment was conducted. A test section for photogrammetry was set up and contained objects such as a bucket, a book, a tennis ball and a bottle.

A typical photograph, as used for photogrammetry, is shown in Figure 46. Old compact discs were used as the control points. These points were measured and used to model the test section.

The procedure as described in paragraph 3.2.1 to 3.2.5 was put into process and a model of the test section was created. The data points were used in Matlab to plot a top view of the test section as well as a three dimensional model. The top view can be seen in Figure 47. A remarkable resemblance between the photograph captured from above and the top view of the model was obtained together with an accuracy of 10 mm. The photograph taken of the test section, shown in Figure 48 compares well the model in Figure 49.

The model of the bottle does not really match the actual bottle. This is due to the height ratios of the camera to the ground and the top of the bottle to the camera. An example in normal photogrammetry with the same problem would be the modelling of a very high and slender building at a rather low flying altitude. This problem does not occur with the bucket because of the cross sectional area of the bucket almost equalling the height. The large ball and small cube seen in Figure 48 were not part of the model in Figure 49.

The results from the test section were satisfactory and it was decided to proceed with the profiling of the Belgian paving at the Gerotek test facilities, utilizing this concept. This is described later in paragraph 5.



Figure 46: Top view of test section as captured with digital camera.

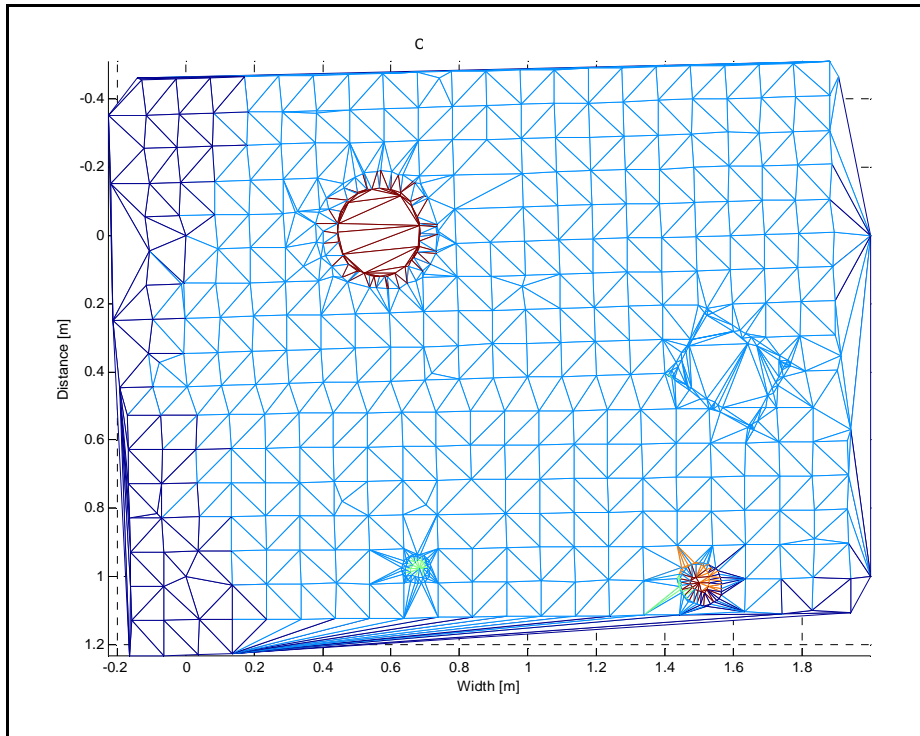


Figure 47: Model of top view for test section.

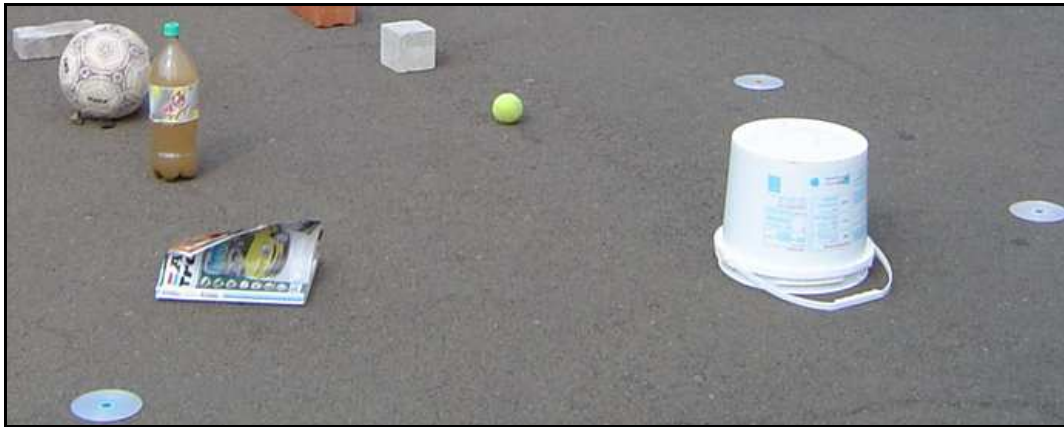


Figure 48: Three-dimensional view of test section.

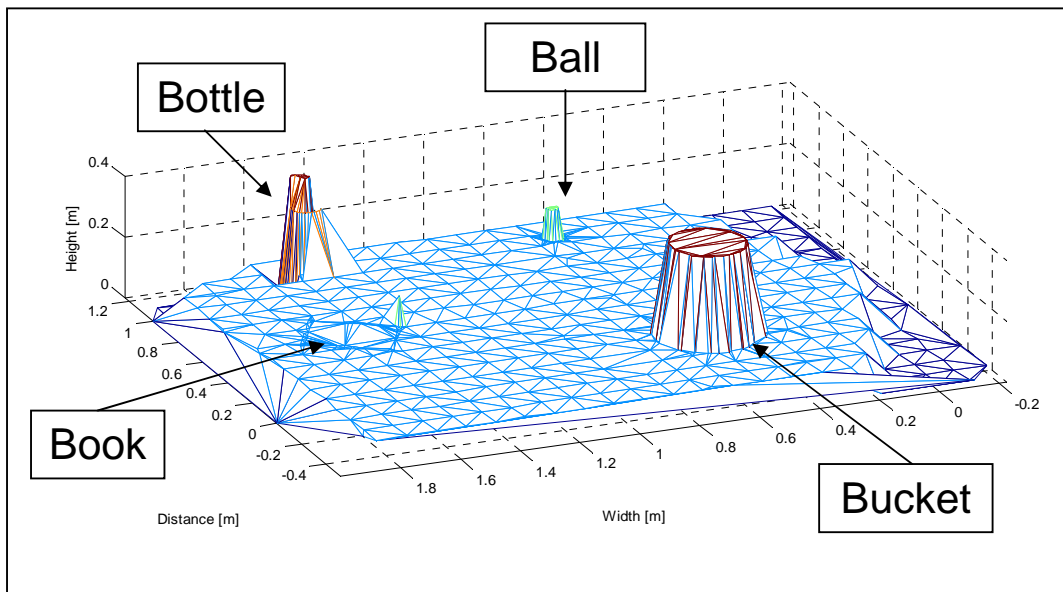


Figure 49: Three-dimensional model of test section.

### 3.3. Laser Scanner

Although commercial 3D laser scanners are available, cost was prohibitive for the purpose of the current study and an in-house system was developed.

The Laser Scanner profilometer utilizes a S80-MH-5 Data Sensor Laser Distance Sensor to measure the profile of the terrain from a vertical distance of 2m. The Data Sensor is mounted in a purposely build gimball which is mounted on a tripod. The gimball enables the Laser Distance Sensor to rotate about two perpendicular axes. The rotation is controlled by two 9438iupf 1.8°/step Stepper motors. A PC 104 data acquisition system controls the stepper motors, measures and saves the angles of the rotations of the stepper

motors and the distance measured by the Laser Distance Sensor from the sensor to the terrain. Figure 50 shows the Laser Distance Sensor and stepper motors mounted on the gimball.



**Figure 50: Gimball containing two stepper motors and a DM-80 Laser Distance Sensor.**

The Laser Distance Sensor can measure a distance from 300 mm up to 4000 mm (on a surface which is from 90% white to 18% grey) with 5 mm accuracy. It is found that the Laser Distance Sensor is very sensitive to the surface to which the measurement is taken. The Laser Distance Sensor has a class 2 laser and the sensitivity on the measured surface is due to the laser only being a 1 milliWatt laser (mW), thus if most of the light is absorbed by the measured surface the laser is incapable of measuring the distance from the lens of the laser to the surface of the terrain. Tests done with and without uv-filters shows that the Laser Distance Sensor does not read any measurement on asphalt terrain whether the asphalt is in a shaded area or in direct sunlight. The Laser Distance Sensor does on the other hand measure on a shaded concrete surface. This means that measurements had to be taken in the dark.

The Laser Scanner profiles a 2.4 x 2.4 m terrain section at a time. If the terrain is viewed from the top, the Laser Scanner starts the profile by saving the angles of the stepper motors and the distance from the Laser Distance Sensor to the terrain, with the Laser Scanner in the centre of the profiled square and on three different corners of the profiled square. The laser is centred by suspending a pendulum from the base of the Laser Distance Sensor. This information is used as the reference from which the rest of the profile is



calculated. The Laser Scanner then moves towards the bottom left corner of the profiled square. Next the Laser Scanner profiles 32 points (referred to as the fast steps) in the positive longitudinal direction (from left to right if viewed from the top) after which the Scanner moves one step in the lateral direction (from the bottom to the top, referred to as the slow steps) and then again scans 32 points in the negative longitudinal direction (right to left).

A 10 second long-exposure photograph captured the movement of the laser and is shown in Figure 51. Figure 52 shows each channel of data as it is recorded. The top graph shows the longitudinal movement of the Laser Distance Sensor and the middle graph the lateral movement. The distance measured from the Laser Distance Sensor to a flat surface is displayed in the bottom graph. The angle of the rotation about both axes is measured with single turn potentiometers on each axis.

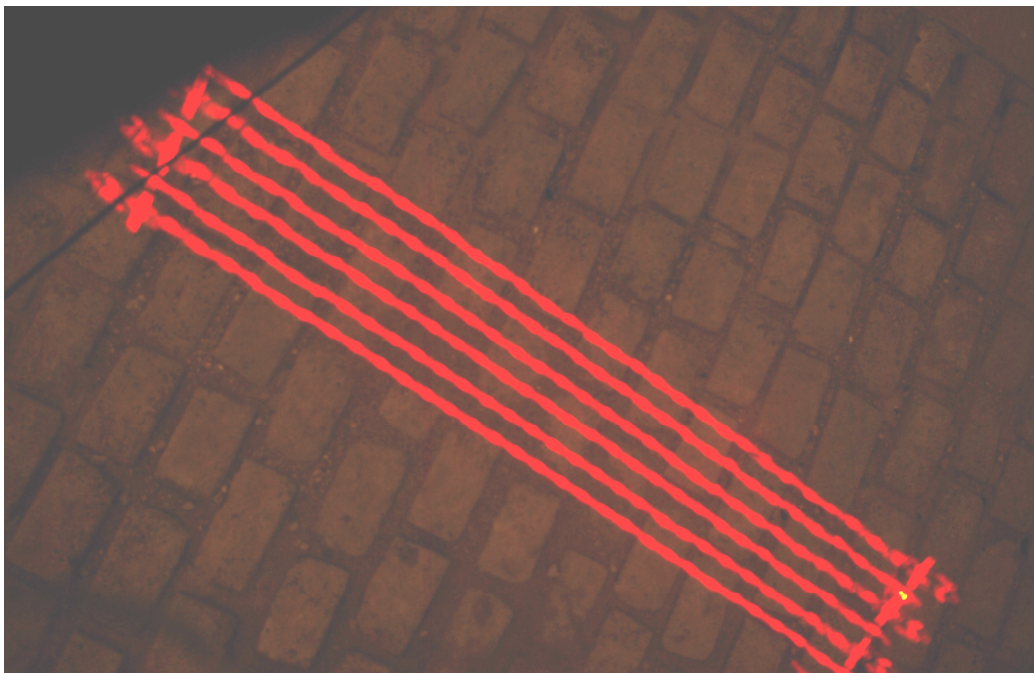


**Figure 51: Top view of the laser movement.**

Figure 53 shows the coordinate system used in calculating the scanned profile. The variables in blue are the measured variables ( $\vartheta, \gamma, L$ ) and the red variables ( $x, y, C, H, \beta$ ) are calculated.

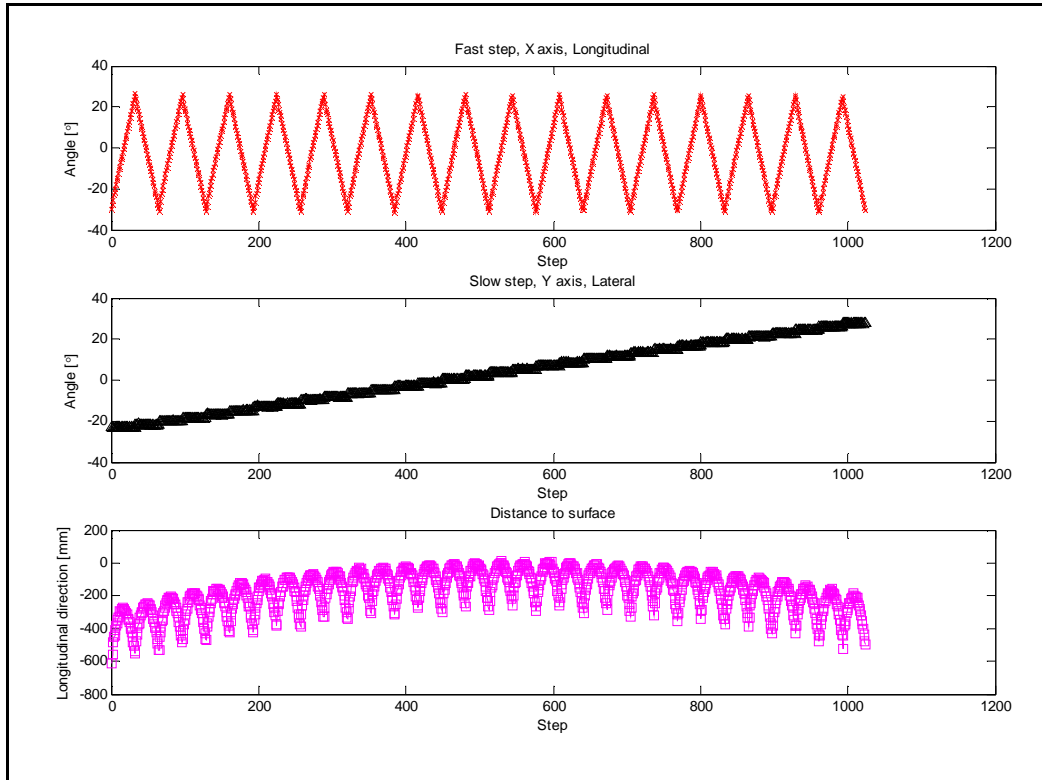


**Figure 52: Measured data of a flat surface.**

The profile of the measured terrain is calculated as follows:

$$\tan \gamma = \frac{y}{H}$$

$$\tan \vartheta = \frac{x}{H}$$

$$\tan \beta = \frac{C}{H}$$

and

$$C = \sqrt{x^2 + y^2}$$

Substituting gives

$$C = \sqrt{\tan^2 \vartheta + \tan^2 \gamma}$$

and

$$\beta = \arctan\left(\frac{C}{H}\right)$$

$C$ ,  $x$  and  $y$  can be calculated independently of  $H$  if the angles are known.

$$H = L \cos \beta$$

$$x = H \tan \vartheta$$

$$y = H \tan \gamma$$

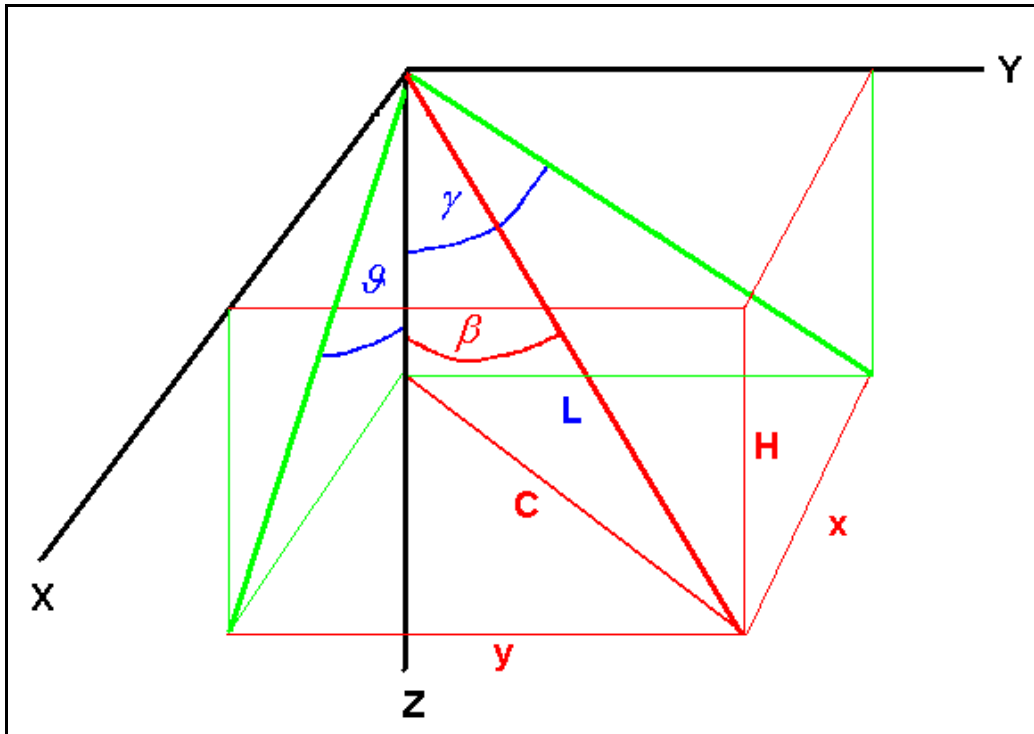


Figure 53: Description of coordinate system used for Laser Scanner calculations.

### 3.3.1. Test section for Laser Scanner

A test was performed on a concrete surface with a 500 x 360 x 58 mm concrete block on it. Figure 54 shows the concrete block on the larger concrete surface.

The surface was profiled at night to ensure that the Laser Distance Sensor was actually measuring correctly. Figure 55 shows the surface as profiled with the Laser Scanner. It can be seen that the profiled surface is slightly convex where the actual surface is flat. This is due to the construction of the gimball. The axis on which the Laser Distance Sensor rotates, goes through the centre of mass and not through the centre of the lens. Thus the lens is moving around instead of remaining in one position and just rotating on the axis. The difference in the position of the axes is added when the profile is determined. The profile is adjusted but some concavity remains. The error is accepted due

to the fact that the profilometer is still a prototype and will be improved in a revised design.

The surface is slightly rougher than the actual terrain because a mesh with an average block size of 60 x 60 mm is obtained with the use of a single step on the stepper motors. The mesh is not equally sized all over because the Laser Distance Sensor is rotated at a constant angle (a single step on the stepper motors). Thus the points neighbouring the centre has a smaller mesh block size and the points near the edge have a larger mesh block size. A smaller mesh may be obtained if reduction gearboxes are integrated onto the stepper motors which will reduce the step to each point.

The accuracy of the Laser Scanner is limited by the gimball, however a revision of the design is required in which the gimball may be revised and reduction gearboxes on the stepper motors incorporated.

The Laser Scanner is used to profile a section of the Belgian paving and is compared with the profiles of the Can-Can Machine and the Photogrammetry in paragraph 5.



**Figure 54: Test block for Laser Scanner with 500 x 360 x 58 mm concrete block on a flat surface.**

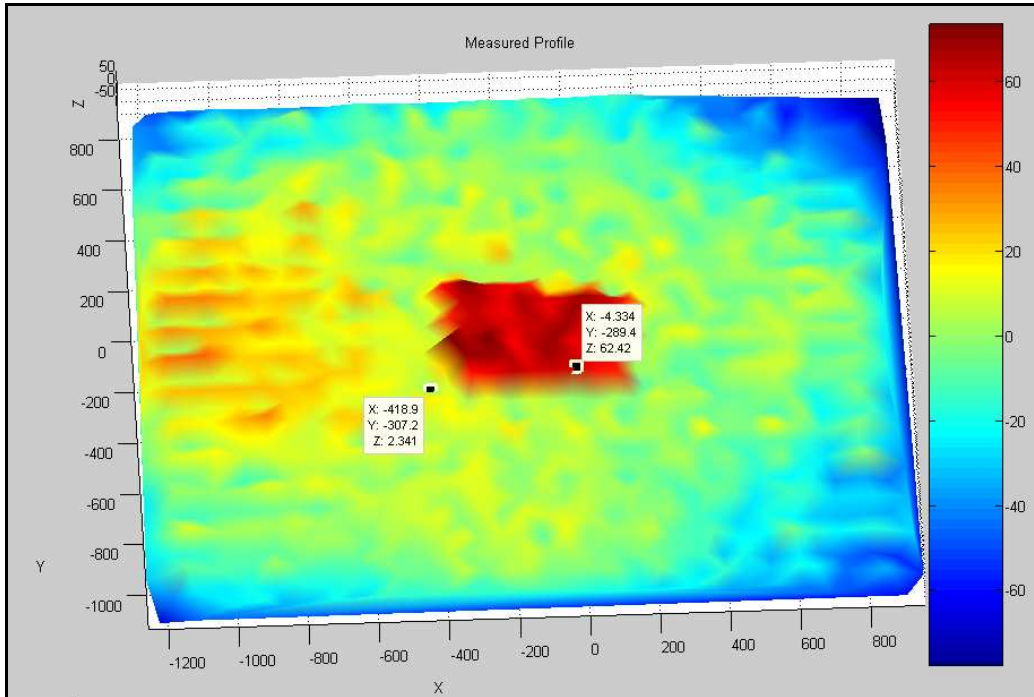


Figure 55: Measure profile of a flat concrete surface with a concrete block on top.

### 3.4. Summary of the three profiling methods

In this paragraph each of the three proposed profilometers were reviewed and the operational functions of each were examined. Test sections were profiled with each of the proposed profilometers and the results were evaluated.

It was found that the Can-Can Machine is a simple and effective profilometer with the ability to profile rough terrain. The Can-Can Machine can profile a terrain with an overall accuracy of < 5 mm. The maximum profiling speed of the Can-Can Machine is 0.98 km/h and produces a profile with a grid size of 100 mm in the lateral direction and 10.18 mm in the longitudinal direction. The width of a Can-Can Machine profile is 3 m.

The Photogrammetric profiling method is a valid and accurate profiling method with an accuracy of 5 mm, however it remains extremely slow and resource intensive. The profiling speed of the Photogrammetric profiling method is in the order of 8 hours/m<sup>2</sup>.

The Laser Scanner is a time consuming Profilometer, however it remains a prospective profilometer still in the development phase. The Laser Distance Sensor has an accuracy of 5 mm but the accuracy of the total system is limited by the gimball. The Laser Scanner profiles with an average longitudinal and lateral resolution of 60 mm and with a total profile width of 2,4 m at a profiling speed of 8 m/hour. The accuracy of the profiler may be improved using a higher quality laser.